Vol. 586: 21–40, 2018
https://doi.org/10.3354/meps12417

MARINE ECOLOGY PROGRESS SERIES
Mar Ecol Prog Ser

Published January 11

Impact of Eastern oyster *Crassostrea virginica* biodeposit resuspension on the seston, nutrient, phytoplankton, and zooplankton dynamics: a mesocosm experiment

Elka T. Porter[1,*], Heather Franz[1], Richard Lacouture[2]

[1]University of Baltimore, Yale Gordon College of Arts and Sciences, 1420 N. Charles St., Baltimore, MD 21201, USA
[2]Patuxent Environmental and Aquatic Research Laboratory, Morgan State University, 10545 Mackall Road, St. Leonard, MD 20685, USA

ABSTRACT: To test the effect of *Crassostrea virginica* biodeposit resuspension on nutrient and plankton dynamics, a 4 wk experiment was performed in six 1000 l shear-turbulence-resuspension-mesocosms (STURM) without a sediment bottom (R). Three tanks (R_BD) received daily additions of oyster biodeposits (5.77 ± 3.33 mg total suspended solids). Simulated tidal resuspension of biodeposits in the R_BD tanks resulted in concentrations of 90 mg l^{-1} total suspended solids when mixing was on, decreasing to ca. 20 mg l^{-1} when mixing was off. However, bulk settling speeds of particles in the R_BD tanks increased 3-fold over the experiment. Particulate nitrogen, phosphorus, and carbon concentrations as well as dissolved inorganic nitrogen, nitrate + nitrite, dissolved organic phosphorus, and total dissolved phosphorus levels were significantly higher in the R_BD tanks. In the R_BD tanks the greatest part (72%) of the nitrogen was partitioned in the total dissolved nitrogen, but in the R tanks the greatest part (51.5%) was partitioned in microphytobenthos. While chlorophyll a concentrations were higher in the R_BD tanks than in the R tanks (despite tunicates being found in the R_BD tanks), phytoplankton biomass (carbon) as estimated using direct cell counts was not significantly different and there was little difference in phytoplankton composition. However, the ratio of chl *a*:C was higher in the R_BD tanks, suggesting phytoplankton adjusted to low light in the R_BD tanks by increasing chl *a* in their cells. *Acartia* sp. abundance was also raised in the R_BD tanks. Addition and regular tidal resuspension of oyster biodeposits profoundly affected nutrient dynamics, nitrogen partitioning, and zooplankton community dynamics.

KEY WORDS: STURM · Biodeposit resuspension · *Crassostrea virginica* · Eastern oyster · Mesocosm · Experimental ecosystem · Benthic-pelagic coupling

INTRODUCTION

In shallow-water ecosystems, benthic and water column environments are closely coupled (Dame 1996). Bivalve filter feeders can play an important role in benthic-pelagic coupling by transferring particles and nutrients from the water column to the sediments in the form of biodeposits (Jordan 1987, Bayne & Hawkins 1992). The introduction of bivalves has been proposed as an additional method to reduce phytoplankton biomass (Dame et al. 1980), suggesting an increase in bivalve populations as a method to restore natural balance to improve water quality in these ecosystems (Cloern 1982, Officer et al. 1982, Cohen et al. 1984, Newell 1988). The use of Eastern oysters *Crassostrea virginica* (Gmelin) to mitigate eutrophication in the Chesapeake Bay has been suggested (Cerco & Noel 2007, Kellogg et al. 2014, Cerco 2015) and the abundance of oysters in the Chesapeake Bay is currently being increased through both

*Corresponding author: eporter@ubalt.edu

restoration (Schulte & Burke 2014) and aquaculture (Williamson et al. 2015, Ray et al. 2015) activities.

The euryhaline, epibenthic, bivalve filter feeder *C. virginica* filters large volumes of water and efficiently filters particles larger than 3 µm from the water column (Haven & Morales-Alamo 1970). Large amounts of feces and pseudofeces as biodeposits reflect a transport of particulate organic matter from the water column to the sediments (Jordan 1987), unless currents resuspend and transport the material (Lund 1957, Widdows et al. 1998). Recent studies have indicated that biodeposits can be resuspended (Colden et al. 2016) and in fact must be transported away from aquaculture sites to avoid deleterious sediment effects (Giles et al. 2009, Testa et al. 2015), such as ammonium effluxes and anaerobic sediments without macrofauna below oyster rafts. Hargrave et al. (2008) developed a nomogram of biogeochemical indicators over an organic enrichment gradient.

It has also been suggested that nutrient regeneration from bivalve biodeposits may counterbalance the removal of phytoplankton biomass by stimulating new phytoplankton blooms (Doering et al. 1986, Asmus & Asmus 1991, Souchu et al. 2001), at least in oligotrophic waters (Cranford et al. 2007). High rates of ammonium flux can occur in sediments underlying natural bivalve populations (Dame et al. 1989, 1991, Asmus & Asmus 1991, Dame & Libes 1993), but other factors such as microphytobenthos abundance also affect nutrient transformations and regeneration (Sundbäck & Granéli 1988, Sundbäck et al. 1991, 2000). Incubation experiments have shown that particulate organic matter, oxygen conditions, and microphytobenthos abundance affect nitrogen transformations and regeneration from the sediments (Caffrey et al. 1993, Enoksson 1993, Newell et al. 2002).

There have been no studies to date that specifically examine interactions between biodeposit resuspension and changes in water quality on oyster reefs or at aquaculture farms. It is generally assumed that oyster biodeposits stay where they fall (Newell et al. 2005, Kellogg et al. 2013). Existing studies of sediment resuspension and benthic processes have shown that resuspension not only enhances nutrient fluxes from sediments (Qin et al. 2004, Almroth et al. 2009, Corbett 2010, Porter et al. 2010, Almroth-Rosell et al. 2012) but also significantly affects microbial and planktonic communities, and thus ultimately biogeochemical cycles (Wainright 1987, 1990, Porter et al. 2010, Isobe & Ohte 2014). While the current focus is primarily on how oysters can fuel the biogeochemically driven nitrogen removal from sediments (Piehler & Smyth 2011, Kellogg et al. 2013, 2014, Smyth et al. 2013), the effect of biodeposit resuspension is less clear. The fraction of deposited material that is resuspended must be known to determine oyster environmental benefits (Cerco 2015).

To study the effects of oyster biodeposits and benthic boundary-layer flow on benthic-pelagic coupling processes in a controllable whole-ecosystem context, 1000 l shear turbulence resuspension mesocosms (STURM) were used. All of the tanks had the same realistic (Porter et al. 2018) volume-weighted water column turbulence levels (RMS turbulent velocity ~1.87 cm s^{-1}, energy dissipation rate ~0.3434 cm^2 s^{-3}) and high area-weighted bottom shear stress (~0.62 Pa). Experiments were run without oysters and without a sediment bottom, and biodeposits collected from oysters (set up separately) were added daily to 3 of 6 tanks.

The specific questions addressed were: (1) How does oyster biodeposit resuspension affect nutrient transformations, nutrient regeneration, and the nitrogen budget? (2) How do resuspended biodeposits affect phytoplankton abundance and composition in whole-ecosystem experiments? (3) How does oyster biodeposit resuspension affect ecosystem processes such as the zooplankton community? Our experiments were designed to determine if the combined effect of high bottom shear stress and oyster biodeposits directly, indirectly, or non-linearly affect ecosystem processes and water quality. The experiment took place at the Morgan State University Patuxent Environmental and Aquatic Research Laboratory, where the outdoor STURM facility is located, from 6 July to 3 August 2016.

MATERIALS AND METHODS

Setup of mesocosms, biodeposit resuspension, and mixing

The experiments reported here primarily focused on water column processes as mediated by biodeposit resuspension and did not use oyster filtration and did not include a sediment bottom. Six cylindrical Shear TUrbulence Resuspension Mesocosms (STURM) tanks (see Fig. S1 in the Supplement at www.int-res.com/articles/suppl/m586p021_supp.pdf) were set up. Each tank contained a single paddle that produced high instantaneous bottom shear stress to resuspend biodeposits and create realistic water column turbulence levels, without overmixing the water column (Porter et al. submitted). The STURM

tanks are the successor design of large linked mesocosms reported by Porter et al. (2004a,b) and are further described by Sanford et al. (2009), Mason & Porter (2009), and Porter et al. (2010, 2013). The mixing goal for this experiment was to set up tidal resuspension where biodeposits would be resuspended during mixing 'on' phases and settling during mixing 'off' phases by keeping water column turbulence levels realistic. Moreover, the goal was to achieve a realistic profile of total suspended solids (TSS) over water column depth: lower near the surface and higher near the bottom.

A single paddle was used that slowly rotated in a forward-stop-backward-stop motion (9 s – 1.5 s – 8 s – 1.5 s) at 18.79 rpm to avoid the entire water column rotating evenly (thus not mixing) during the mixing 'on' phase. Mixing was turned on for 4 h and off for 2 h in all systems to simulate tidal cycles throughout a 4 wk experiment. The tanks had a water volume of 1000 l, a water column depth of 1 m, and a sediment surface area of 1 m^2, but contained no sediment for this experiment. Three tanks each received a daily addition of oyster biodeposits (5.8 ± 3.3 mg TSS daily) starting in the afternoon of Day 2 of the experiment. Biodeposits were generated in an oyster holding area separate from the experiment using natural plankton in flow-through conditions.

Direct flow and turbulence measurements were made using a Sontek 10 Mhz Acoustic Doppler Velocimeter to determine water column RMS turbulent velocity and energy dissipation rates at predefined locations throughout the tank, and at different mixing speeds. RMS turbulent velocity is defined in Tennekes & Lumley (1972) as:

$$q = \sqrt{\frac{1}{3}(< u^2 > + < v^2 > + < w^2 >)} \quad (1)$$

where $<u^2>$, $<v^2>$, and $<w^2>$ are the variances of their respective velocity components. Energy dissipation rates were determined following Sanford (1997). Volume-weighted average RMS turbulent velocities as determined using Surfer (Golden Software) were ~1.87 cm s^{-1} (Fig. 1a), which are at the low end of values measured in continental shelf benthic boundary layers (Heathershaw 1976). Volume weighted energy dissipation rates were ~0.3434 cm^2 s^{-3} during mixing (Fig. 1b), similar to values found in continental shelf benthic boundary layers (Gross et al. 1994) or near the surface at breaking waves (Terray et al. 1996). Energy dissipation rate was about

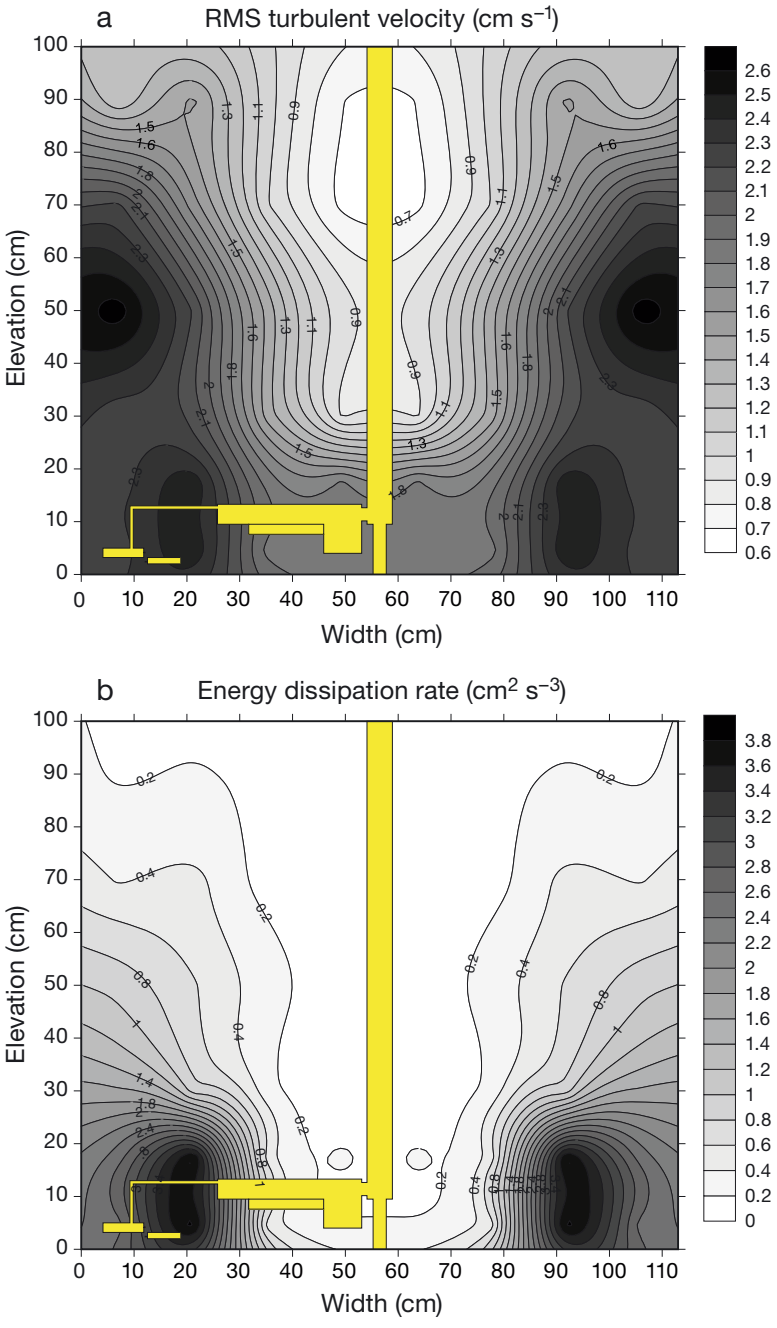

Fig. 1. Distribution of (a) turbulence velocity (q) and (b) energy dissipation rate during mixing 'on' phases in all systems. The STURM mixing paddle is shown in yellow

half as high as in the high mixing treatment of Petersen et al. (1998). These turbulence levels are slightly higher than used in previous experiments comparing resuspension vs. non-resuspension systems (Porter et al. 2010) and in linked mesocosms (Porter et al. 2004a,b), but are in the realistic range (Porter et al. 2018, Table 1 in Sanford 1997). This mixing setting kept energy dissipation rates, which are non-linearly related to RMS turbulent velocity (Sanford 1997), at realistic levels (Porter et al. 2018).

Shear stress was determined at the bottom of the tank by using hot film anemometry (Gust 1988). Shear (or 'friction') velocity (u_* in cm s^{-1}), defined by:

$$u_* = \sqrt{\frac{\tau_b}{\rho}} \quad (2)$$

where τ_b is bottom shear stress in dynes cm^{-2}, and ρ is the density of water in g cm^{-3}, was measured at 5 locations across the tank radius. Bottom shear stress [Pa] was calculated as:

$$\tau_b = \frac{u_*^2 \rho}{10} \quad (3)$$

At the chosen mixing setting, area-weighted maximum instantaneous bottom shear stress reached 0.62 Pa in all tanks (Fig. 2) and produced biodeposit resuspension in the R_BD tanks during the mixing 'on' phases, while settling occurred during the mixing 'off' phases (Fig. 3) over a 4 wk period. These shear stress levels are found in continental shelf and microtidal estuarine benthic boundary layers (Grant et al. 1984, Sanford & Halka 1993, Gross et al. 1994) and macrotidal estuarine boundary layers (Wright et al. 1992, Johnson et al. 1994). In addition, a vertical profile of TSS concentration over water column depth was measured to be similar to profiles in estuaries (e.g. Liu et al. 2014) when shear stress is high enough to resuspend sediments off the bottom and move them up into the water column (Fig. 4).

The tanks were wrapped in aluminum-coated reflective bubble wrap (Shelter Institute) to reduce overheating of the tank water during high outdoor summer temperatures (up to 38°C). In addition, 2 layers of window screen mesh were placed over the superstructure to reduce insolation, ~1.5 m above the tanks.

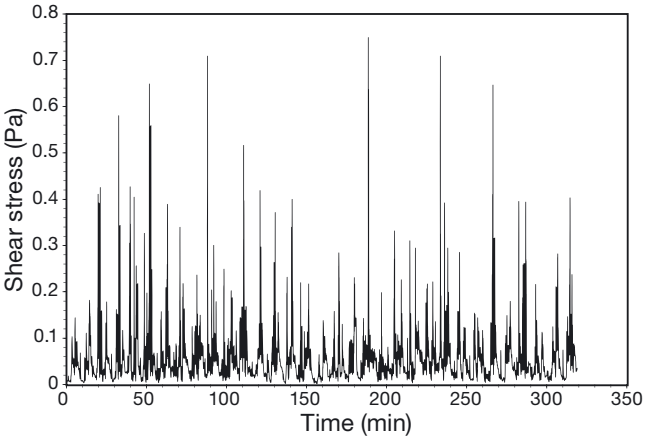

Fig. 2. Bottom shear stress during mixing 'on' phases in all systems. Shown is data from 1 of 6 shear stress sensors distributed radially across the bottom of a STURM tank. Data from all sensors were area-weighted

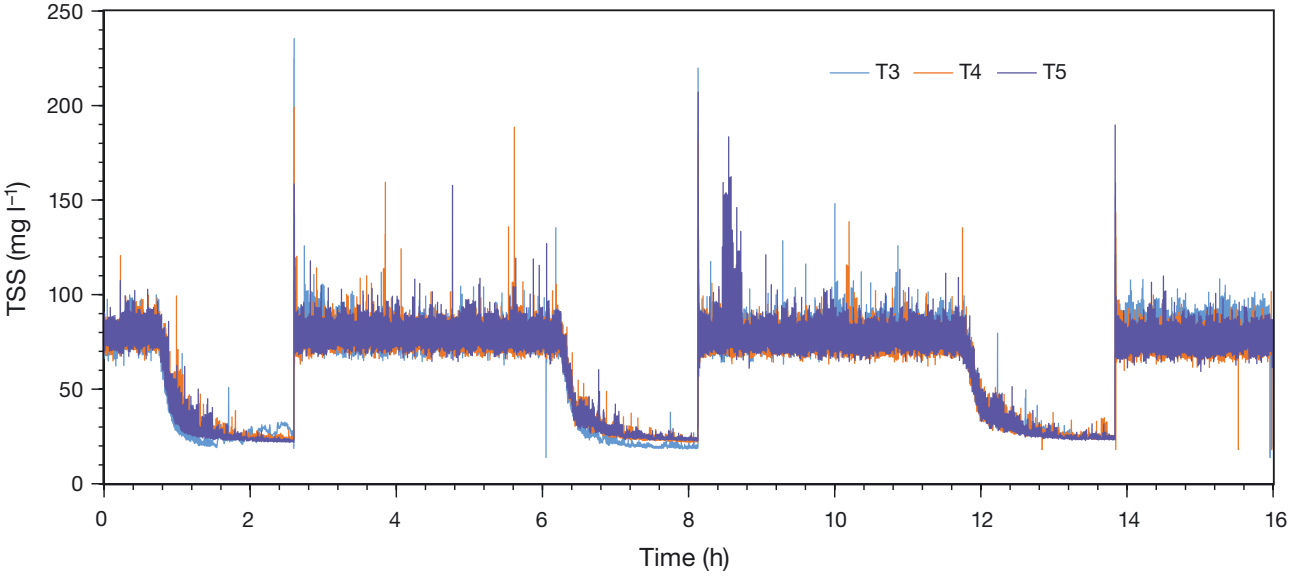

Fig. 3. Tidal resuspension of biodeposits with resuspension and settling of total suspended solids (TSS) in the 3 R_BD tanks (T3, T4, and T5) from 31 July to 1 August 2016 as measured with OBS-3 turbidity meters

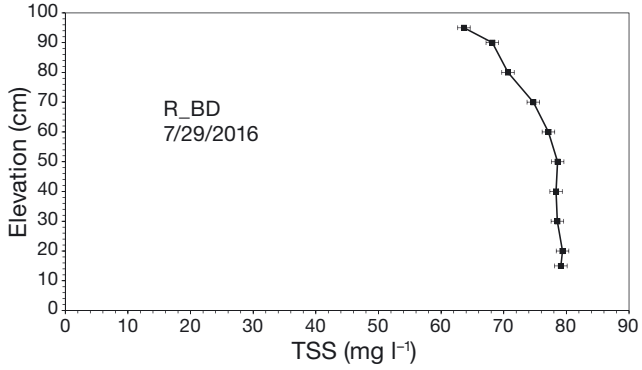

Fig. 4. Vertical profile of TSS concentrations in the R_BD tanks on 29 July 2016 generated from OBS-3 turbidity profiles. Averages of 3 tanks ± SD

The tanks were slowly and evenly filled with unfiltered 12.9 g kg^{-1} salinity water containing the resident plankton community from the Patuxent River, a tributary of Chesapeake Bay. Only megazooplankton were excluded. Mixing began with the programmed tidal cycles and all tanks were synchronized. The experiment took place over 28 d, from 6 July 2016 to 3 August 2016.

Ten percent of the water in each tank was exchanged daily at the end of the mid-day mixing 'off' phase to mimic tidal exchange and replaced with 0.5 µm absolute filtered Patuxent River water. Filtered water was used for the exchange (e.g. Porter et al. 2004a,b, 2010, 2013). Any nutrients added with the fill water were accounted for in the nitrogen budget. The tank walls were cleaned of periphyton daily to minimize wall growth (Chen et al. 1997) and the wall material was left in the tank to avoid affecting any mass balances (Porter et al. 2004b, 2010, 2013).

Biodeposit additions

Starting on Day 2, equal amounts of oyster *Crassostrea virginica* biodeposits were added to each of 3 R_BD tanks during the late afternoon mixing 'on' phase. The sampling of particulates and nutrients on Day 2 was done in the morning before any biodeposits had been added to the tanks and reflects all tanks without any biodeposit additions. Oyster biodeposits were collected daily from 218 oysters (10.4 ± 1.7 cm long) held in flow-through conditions of ambient Patuxent River water in an indoor raceway. Thus, biodeposits from 72.7 oysters m^{-2} were added to each tank daily. Total suspended solids (TSS), particulate inorganic matter (PIM), particulate organic matter (POM), and quality (ratio POM/PIM) of the biodeposits added were determined daily. Particulate carbon (PC), particulate nitrogen (PN), chlorophyll *a* (chl *a*), and phaeophytin concentrations were determined every 2 d. On average 5.8 ± 3.3 g TSS, 632 ± 365 mg PC, 76.5 ± 50.1 mg PN, 14.9 ± 9.2 mg particulate phosphorus (PP), 1.42 ± 0.83 mg chl *a*, and 6.3 ± 3.5 mg phaeophytin in the biodeposits were added daily to each tank, i.e. per m^{-2}, with a ratio of POM to PIM of 0.6 ± 0.2. Newell et al. (2002) define low, medium, and high biodeposit additions as 0.25, 2.5, and 5 g C m^{-2} d^{-1}, respectively, and our biodeposit additions were in the medium range.

Temperature, salinity and dissolved oxygen

Dissolved oxygen concentrations were measured daily during mixing 'on' phases in the afternoon at mid depth using a YSI 95 sonde. Water temperature was measured at 10 min intervals in all tanks over the experiment using Campbell T107 temperature probes connected to a Campbell CR10× data logger (Campbell Scientific). The 6 tanks tracked each other closely, and the Campbell temperature data were analyzed in detail to determine the temperature variability in the systems. During Week 3, during a heat wave, temperatures in the tanks were compared daily to water temperatures in a shallow local Patuxent River cove. The temperatures were similar, and no cooling intervention took place to further cool the tank water. Silver bubble wrap and 2 layers of window screen above the tanks were sufficient to shield the tanks from excessive heat. Salinity was measured weekly using a refractometer.

TSS, particle settling, particulate and dissolved nutrients

Geochemical variables measured included TSS concentrations, particulate nitrogen (PN), particulate carbon (PC) and particulate phosphorus (PP) concentrations, as well as water column dissolved nutrient concentrations (ammonium, nitrate plus nitrite, dissolved inorganic nitrogen [DIN], phosphate, total nitrogen [TN], and total phosphorus [TP]) measured biweekly during morning mixing 'on'. Particulates were also measured during the mixing 'off' that followed on Days 13, 20 and 27. Particle bulk settling speeds were measured during the mid-day mixing 'off' phases in the R_BD tanks using optical backscatter (OBS-3) turbidity data.

Turbidity was measured continuously at 1 s intervals in each tank with optical backscatter (OBS-3, D&A Instrument Company) turbidity sensors located at mid-depth. Turbidity was calibrated with concurrently collected mid-depth TSS samples, analyzed by filtration and weighing as described below. In post-processing, OBS data were averaged over 66 s intervals.

Water was filtered through pre-ashed, pre-weighed 47 mm Whatman GF/F filters (0.7 µm nominal pore size) and rinsed with an isotonic solution of ammonium formate to remove salts (Berg & Newell 1986). To determine TSS mass, filters were weighed on a Mettler AE 240 microbalance after drying for 24 h to constant weight at 60°C. Then the filters were ashed at 450°C for 4 h and re-weighed to determine particulate inorganic matter (PIM) concentrations. Particulate organic matter (POM) was determined by the difference between TSS and PIM (Berg & Newell 1986).

Known volumes of water were filtered through 47 mm Whatman GFF filters for particulate phosphorus (PP). In addition, water was filtered through pre-ashed 25 mm Whatman GFF filters to measure particulate nitrogen (PN), and particulate carbon (PC) concentrations. Nutrients and water column chl *a* and phaeophytin were analyzed by the Analytical Services Laboratory, University of Maryland Center for Environmental Science (Chesapeake Biological Laboratory Analytical Services Laboratory 2017a,b). Water samples were analyzed for particulate phosphorus (PP) following Environmental Protection Agency (EPA) Method 365.1 'ASPILA' (1979). Particulate carbon (PC) and nitrogen (PN) samples were analyzed on a Model CE-440 Exeter Analytical (CHN) analyzer using EPA Method 440.0 (Zimmerman et al. 1997). The solute was captured and frozen in individual vials until it was analyzed for dissolved nutrients including ammonium (NH_4^+), nitrate + nitrite (NO_3^- + NO_2^-), dissolved phosphate (PO_4^{3-}), dissolved silicate (Si), total dissolved nitrogen (TDN) concentrations, and total dissolved phosphorus concentrations. Ammonium (SM 4500-NH3 G-1997), nitrite plus nitrate (ASTM D-7781, EPA 352.2 Cadmium), and phosphate were analyzed on a Konelab Aquakem 250 multi-wavelength automated discrete photometric analyzer, and total dissolved nitrogen and phosphorus were analyzed using EPA Method 353.2 and EPA Method 365.1, respectively. Dissolved organic phosphorus (DOP) was calculated by the difference between total dissolved phosphorus and phosphate (PO_4^{3-}). Dissolved organic nitrogen (DON) was calculated by the difference between TDN and dissolved inorganic nitrogen (DIN). Dissolved silicate was analyzed using a Konelab Aquakem 250 multi-wavelength automated discrete photometric analyzer with oxalic acid added to minimize interference from phosphates (EPA Method 366.0, 1997). For quality control of all variables, each sixth sample was analyzed in duplicate.

Exchange water was also sampled for dissolved nutrients to track any nutrient inputs through a 10% daily water exchange. In addition, the fill water was sampled for particulates to confirm that their abundance in the fill water was low (8.3 ± 4.7 mg l^{-1}). The same techniques were used to analyze particulates in the biodeposits. Duplicate subsamples were analyzed randomly for quality control during each sampling.

During each water sampling, the exact times of sampling for each OBS-3 turbidity meter were recorded to establish linear calibration curves of TSS versus OBS volts. The linear calibrations for each OBS-3 turbidity meter (TSS = 135.5 × OBS_V + 13.941, R^2 = 0.94; TSS = 1122.87 × OBS_V + 15.486, R^2 = 0.93; TSS = 60.53 × OBS_V + 19.324, R^2 = 0.92) were used to determine TSS concentrations in the tanks from continuous OBS turbidity measurements.

Bivalves repackage organic matter into biodeposits, and we expected the size structure and settling of the particles to be different in the R_BD compared to R tanks. Bulk particle settling speed (mm s^{-1}) was measured in the 3 R_BD tanks using the settling profiles generated by the OBS-3 turbidity meters during mixing-off phases. We used the distance from the surface to the turbidity sensor (0.5 m depth) divided by the time to reduce the initial TSS concentration by 50% of the range to its steady state value. TSS concentrations measured 3 times during the mixing 'on' and mixing 'off' phases during the experiment were not significantly different in the R tanks, particles did not settle, and, thus, no bulk settling speeds were determined in the R tanks. More frequent samples of TSS, PIM, POM, POM:PIM, PN, PP, PC, and chl *a* were collected during 3 mixing off periods on Days 13, 20, and 27 to examine changes in the particulate properties over time during settling.

Profiles of TSS concentrations over tank depth were determined 6 times over the experiment during the mixing 'on' phases. OBS readings, calibrated for TSS, were taken for 5 min each at 5, 10, 20, 30, 40, 50, 60, 70, and 80 cm from the surface. This was as close to the bottom as possible without interfering with the paddle. TSS concentrations over depth were graphed

and increased with increasing depth until ~50 cm and then stayed constant to 80 cm.

Phytoplankton, light, microphytobenthos

Biological variables measured included water column chl *a*, phaeophytin, phytoplankton identification, and cell count measured biweekly and during 3 mixing 'off' times on Day 13, 20, and 27. In addition, light profiles, Secchi depth, and sediment chl *a* and microphytobenthos pigments were measured. Known volumes of water were filtered through 47 mm Whatman GF/F filters for chl *a* and phaeophytin concentrations. Chl *a* concentrations were measured using fluorometric techniques without acidification (Welschmeyer 1994) after extraction with 90% acetone to provide estimates of phytoplankton biomass. Phaeophytin was measured following EPA Method 445. In addition, water subsamples were preserved biweekly in Lugol's iodine solution for later microscopic phytoplankton identification and cell counts. Phytoplankton cells were counted using Utermöhl procedures (Marshall & Alden 1990, Lacouture 2001). Phytoplankton biomass was determined by converting mean cell volumes of individual taxa to cell carbon according to Smayda (1978) and Strathmann (1967). To determine if the light regime in the R and R_BD tanks affected phytoplankton, the ratio of chl *a*:phytoplankton carbon was determined.

For the first 4 d of the experiment, an intensive study of surface irradiances was carried out at each of 4 quadrants in each tank to determine if the mesh cover was limiting light and to determine the most representative location in each tank to measure light profiles. Light levels of ~255 µmol photons m^{-2} s^{-1} were measured at the water surface of the R tanks and R_BD tanks, using a LI-192 Underwater Quantum sensor (LI-COR Biosciences) attached to a model LI-250 readout. In previous experiments, it was found that light levels of ~160 µmol photons m^{-2} s^{-1} are required at the water surface to prevent light limitation (Porter et al. 2004b). Therefore, any light limitation within the tanks was due to the impact of biodeposit resuspension and/or the density of phytoplankton that resulted.

Subsequently, light profiles were measured twice a week during mixing 'on' and 'off' phases measuring the total downwelling photosynthetically active radiation (PAR, in the 400 to 700 nm waveband) at 0, 10, 25, 50, and 60 cm from the water surface. Light attenuation coefficients were determined and irradiance levels at the tank bottom calculated. In addition, the mean geometric irradiance was calculated in the water column as:

$$\text{Mean geometric irradiance} = \exp[0.5 \times \{\ln(E_0) + \ln(E_{Sed})\}] \quad (4)$$

where E_0 and E_{Sed} are irradiances at the surface of the water column and the bottom, respectively. The values obtained for mean geometric irradiance were similar to irradiance values measured at 50 cm depth. Secchi depth was measured almost daily during the mixing 'on' and 'off' phases using a PVC cap painted black and white, similar to a Secchi disk, mounted onto a PVC rod and lowered into the water column until it disappeared from view.

Sediment chl *a*, and microphytobenthos pigment concentrations were measured at the end of the experiment. Using razor blades, microphytobenthos was scraped off duplicate 4 cm × 15 cm and 10 cm × 4 cm fiberglass plates that were affixed with aquarium sealant to the tank bottoms at 0–10 cm from the outer wall and 20–35 cm across the radius of the tanks before the experiment to allow easy removal of microphytobenthos. Sediment pigment samples were frozen at −70°C pending analysis with high performance liquid chromatography (HPLC; Van Heukelem & Thomas 2001). Microphytobenthos pigments were extracted by adding acetone to the sample containers, transferring the sample to sample tubes, and sonicating each tube at 0°C. The supernatant was decanted after centrifugation and subsequently analyzed by HPLC. HPLC was used to prevent interference from degradation products such as chlorophyllides and phaeophorbides that interfere with fluorescence measurements (MacIntyre et al. 1996) and affect chl *a* readings. Chlorophyllides and phaeophorbides can be abundant in areas with bivalves (e.g. Karakassis et al. 1998). The level of chl *a* without degradation products was determined by subtracting phaeophytin and phaeophorbide from total chl *a*. The ratio of 19′ Butanoyloxyfucoxanthin, 19′ Hexanoyloxyfucoxanthin, Alloxanthin, Diadinoxanthin, Diatoxanthin, Fucoxanthin, Peridinin, Zeaxanthin, Lutein, and Violaxanthin to chl *a* was determined to see if there were differences between the microphytobenthos community in the R and R_BD tanks at the end of the experiment. Due to the difficulty in the transfer of solute from the original sample containers of R tanks to the sonication tube, it is not clear if all pigment was conveyed, and the microphytobenthos biomass is likely underestimated in the R tanks.

Mesozooplankton and macrofauna

Biological variables measured included mesozooplankton abundance and species composition as well as macrofauna abundance. Mesozooplankton were sampled twice a week during mixing 'off' by pumping 40 l tank^{-1} at 27 l min^{-1} through a 63 µm Nitex screen, using a diaphragm pump. The samples were washed into bottles and preserved with buffered formaldehyde. The dominant taxa in the mesozooplankton and age groups were determined on a dissecting microscope using direct counts. To estimate the dry weights of the different taxa, the number of individuals was multiplied by their taxon's respective weight characteristic (Table 2 in White & Roman 1992; *W*, µg ind^{-1}). Thus, the number of adult *Acartia tonsa* for each sampling day was multiplied by 8, the number of polychaete larvae by 1.3, the number of copepodites by 2.7, the number of copepod and barnacle nauplii by 0.31, the number of barnacle cyprids by 2.8, crab zoea by 20 (Torres et al. 2002) and veliger larvae by 0.1342 (Sprung 1984). The dominant taxa were copepod nauplii, *Acartia* sp. adults, polychaete larvae, and copepodites.

Zooplankton densities (ind. l^{-1}) were converted to carbon (µg l^{-1}) for each taxon, and the taxa were combined for an estimate of combined mesozooplankton biomass to compare their relative biomass to phytoplankton abundance (in a common carbon unit) following White & Roman (1992, their Table 1: 'Carbon [µg C ind.$^{-1}$] = 0.32 *W*'). In addition, the nitrogen content of the zooplankton community was estimated for an overall nitrogen budget as described with the nitrogen budget below.

Unexpectedly, adult polychaetes had built burrows in the microphytobenthos mat at the end of the experiment in the R tanks. In addition, tunicates *Molgula manhattensis* were found in the R_BD tanks. Thus, to determine the abundance of macrofauna that may have settled or grown up over the 4 wk period of the experiment, a diaphragm pump was used to suction up the bottom half diameter of each tank after emptying the tank to a water depth of ca. 2 cm. The contents were washed through a 0.5 mm diameter mesh and the macrofauna preserved with buffered formaldehyde. *Molgula manhattensis* has been reported to filter 540 ml h^{-1} per g wet weight (Millar 1971). The wet weight of 10 tunicates was determined and averaged to result in 0.152 g ind.$^{-1}$ wet weight. The amount of water filtered per day by the tunicates was determined.

Nitrogen budget

In estimating nitrogen budgets in the R and R_BD tanks, water-column phytoplankton direct cell counts were converted to phytoplankton carbon after Smayda (1978) and Strathmann (1967), and the Redfield ratio of C:N of 106:16 was used to convert phytoplankton to nitrogen equivalents.

Average sediment chl *a*, indicative of microphytobenthos abundance, was converted to nitrogen equivalents (g N per tank) after converting mg chl *a* m^{-2} to µg chl *a* m^{-2}. To convert chl *a* biomass, a POC to chl *a* ratio of 51.68 was used (Porter et al. 2010). In addition, the measured carbon to nitrogen ratio of 5.138 from Porter et al. (2010) was used. The nitrogen estimate of microphytobenthos is likely an underestimate in the R tanks because microphytobenthos was probably underestimated. To estimate the nitrogen content of the zooplankton community, we determined the dry weights of the individuals of the different taxa following White & Roman (1992), Torres et al. (2002) and Sprung (1984), then the numbers were scaled up to total dry weight in the tanks using measured abundances. The nitrogen content of the mesozooplankton stock in the tanks was considered to be 7.5% of the mesozooplankton dry weight (5 to 10% of mesozooplankton dry weight is nitrogen; Parsons et al. 1984). Water-column concentrations of TDN were corrected for the daily water exchange and scaled up to the whole tank.

Statistical analyses

After Porter et al. (2010, 2013), chl *a*, phaeophytin, total suspended solids, the dissolved inorganic and organic nutrients, and particulate nitrogen, phosphorus, and carbon were each averaged from Day 2 to Day 27 of the experiment for each tank (8 measurements over a 4 wk period) and also analyzed without Day 2 as noted below, because no biodeposits had been added to the tank yet at the Day 2 sampling. The mesozooplankton abundance was averaged for each tank from Day 3, the first time of zooplankton measurement, to Day 28. Only data from the mixing 'on' phases were included in statistical comparisons. Statistical *t*-tests were used for water column chl *a*, phaeophytin, PN, PC, the dissolved nutrient data, the dissolved oxygen, zooplankton abundance, and the microphytobenthos accessory pigment to chl *a* ratio. We used linear regression analyses of mesozooplankton biomass and phytoplankton biomass (estimated from direct cell counts) to determine the relationship between the

mesozooplankton community and phytoplankton. Statistical analyses were performed using SAS (SAS Institute), and the *t*-tests using the Microsoft Excel Analysis tool pack. Significances of all analyses were defined at the $p \leq 0.05$ level. Results over the whole datasets are reported here, including sampling Day 2 before biodeposits were added, except where noted.

RESULTS

Temperature, salinity, and dissolved oxygen

Water temperatures ranged from 25.8 to 30.8°C in the R tanks (average 28.09 ± 0.11°C) and from 25.4 to 30.5°C (average 27.88 ± 0.189°C) in the R_BD tanks, and Days 19 to 23 experienced a heat wave. Dissolved oxygen concentrations were significantly lower in the R_BD tanks compared to the R tanks (Fig. 5). Salinity ranged from 11 to 12 ppt over the course of the experiment.

TSS, particle settling, particulate and dissolved nutrients

Total suspended solids (TSS) concentrations were significantly higher in the tanks with oyster *Crassostrea virginica* biodeposits (R_BD; ~95 mg l^{-1} in Week 3; Fig. 6a) than in the resuspension tanks without added biodeposits (~15 mg l^{-1}; Fig. 6a, Table 1). In the morning of Day 2 of the experiment, before biodeposits were added, TSS concentrations were 13.94 ± 0.70 mg l^{-1} and 13.39 ± 4.15 mg l^{-1} in the R tanks and R_BD tanks, respectively, and not significantly different ($p = 0.841$). Throughout the experiment, TSS concentrations continuously increased in the R_BD tanks to ~95 mg l^{-1}, until they started to decrease somewhat towards the end of the experiment (Fig. 6a). During mixing 'off' phases, TSS concentrations were about 15 to 20 mg l^{-1} in both the R_BD and the R tanks (Fig. 6a,b).

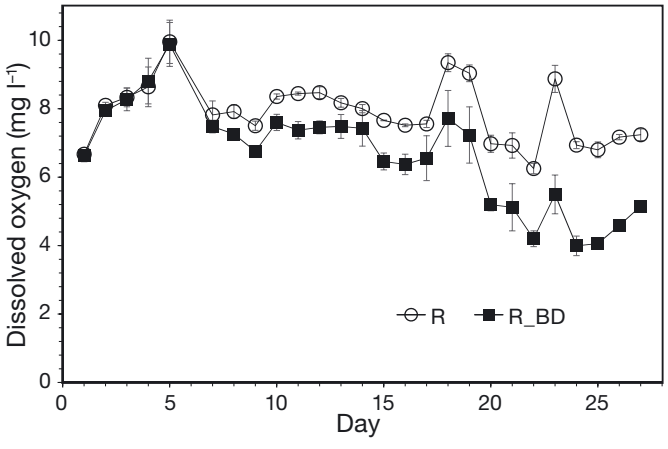

Fig. 5. Dissolved oxygen concentrations measured in all tanks over the experiment. Averages of 3 tanks ± SD

TSS concentrations were the same between mixing 'on' and 'off' phases in the R tanks (Fig. 6a,b), and particles did not settle. Bulk settling speeds changed in the R_BD tanks over the course of the experiment (Fig. 7). On Day 2, bulk settling speed was only approximately 0.07 mm s^{-1} and hardly any particle settling occurred; however, between Day 3 and 13, bulk settling speeds rose to 0.44 ± 0.17 mm s^{-1}, and after Day 15, it greatly increased to 1.30 ± 0.09 mm s^{-1} for the remainder of the experiment in the R_BD tanks (Fig. 7).

Particulate carbon (PC), nitrogen (PN), and phosphorus (PP) concentrations were linearly related to TSS concentrations: PC (mg l^{-1}) = 0.1166 × TSS (mg l^{-1}) − 0.7515, $R^2 = 0.97$; PN (mg l^{-1}) = 0.0158 × TSS (mg l^{-1}) − 0.0876, $R^2 = 0.97$; PP (mg l^{-1}) = 0.0028 × TSS (mg l^{-1}) − 0.0225, $R^2 = 0.96$. PC and PN concentrations were significantly enhanced in the R_BD tanks (Fig. S2a–f, Table 1). Much of the PN, PC, and PP settled out during mixing 'off' phases in the R_BD tanks (Fig. S2b,d,f in the Supplement).

Defining nutrient limitation as dissolved silicate < 5 µmol l^{-1}, DIN < 2 µmol l^{-1}, and phosphate < 0.1 µmol l^{-1} (Fisher et al. 1992, T. Fisher pers. comm.), all nutrients except silicate became limiting in the R tanks after Day 4 (Fig. 8c,e,g), and silicate became limiting after Day 16. In the R_BD tanks, silicate was never limiting and DIN and phosphate were limiting from Day 4 to 14. However, nutrient addition bioassays such as used by Fisher et al. (1999) would be needed to determine the limiting nutrient. Dissolved organic phosphorus concentrations were significantly higher in the R_BD tanks (Fig. 8h, Table 1).

While total nitrogen ($NH_4^+ + NO_2^- + NO_3^- +$ DON + PN) concentrations were about the same in all tanks at the beginning of the experiment and stayed at ~40 µmol l^{-1} in the R tanks for the duration of the experiment, they increased steadily in the R_BD tanks until Day 22 after which they decreased (Fig. 8f, Table 1e). Total phosphorus concentrations (PO_4^{3-} + DOP + PP) were ~1.5 µmol l^{-1} in all tanks at the beginning of the experiment and stayed the same in the R tanks over the experiment. In the R_BD tanks, total phosphorus concentrations increased until about Day 22 and then decreased (Fig. 8i). The ratio of TN:TP was significantly lower in the R_BD tanks than in the R tanks (Fig. 8l, Table 1). The patterns of TP and TN progressions were similar to the patterns

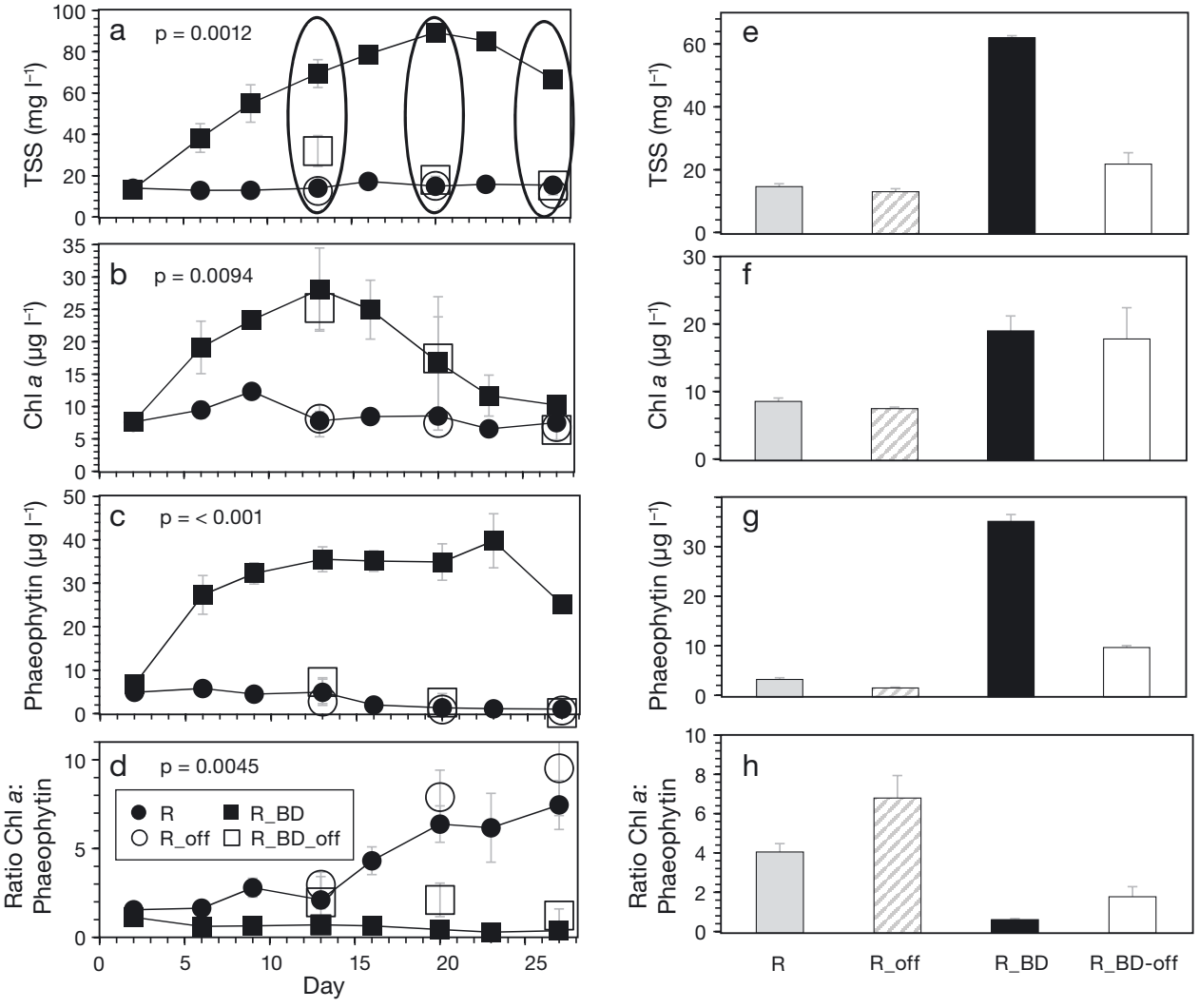

Fig. 6. Left panels: time series of 4 variables; right panels: data from R and R_BD tanks for mixing 'on' and mixing 'off' phases averaged over 3 of the days, as indicated by ellipses in panel (a). (a) Total suspended solids (TSS), (b) chlorophyll *a* concentrations, (c) phaeophytin concentrations, (d) ratio of chl *a*:phaeophytin over the experiment. (e) TSS, (f) chl *a*, (g) phaeophytin and (h) ratio of chl *a*:phaeophytin during mixing 'on' and mixing 'off' phases. Means and SD (n = 3)

of the TSS concentrations over time, suggesting that resuspended biodeposits may have been a source of additional nutrients. Most of this increase in TP was due to resuspended PP, which was related linearly to TSS levels. Most of the increase in TN was due to resuspended PN, which was related linearly to TSS levels.

The switch to increased bulk settling speeds after Day 15 coincided with the start of an increase in phosphate, DIN, and nitrate + nitrite concentrations that lasted for the remainder of the experiment (Fig. 8). In addition, this increase in nutrient concentrations overcame nutrient limitation in the R_BD systems (Fig. 8) and increased as chl *a* concentration decreased (Fig. 6c).

Nutrient concentrations were consistent with the differences for chl *a* (Fig. 6c, Table 1). Nitrate plus nitrite concentrations (Fig. 8d), dissolved phosphate (PO_4^{3-}) concentrations (Fig. 8e), total dissolved nitrogen, and phosphorus concentrations (Fig. 8f,i) were significantly higher in the R_BD tanks than in the R tanks (Fig. 8, Table 1), and DON concentrations were similar (Table 1, Fig. 8j). As chl *a* increased in the R tanks (Fig. 6a), $NO_2^- + NO_3^-$ (Fig. 8b), NH_4^+, and dissolved PO_4^{3-} (Fig. 8a,e) decreased. However, midway in the experiment, chl *a* concentrations decreased as nutrient concentrations increased. While nutrient concentrations were related to the chl *a* concentrations in the R and R_BD tanks, they did not relate to phytoplankton direct cell counts.

Table 1. Summary of statistical results for the resuspension (R) and resuspension with biodeposit addition (R_BD) systems, mixing 'on' phases. Statistical *t*-tests used in all analyses. Significance was defined as $p \leq 0.05$. Means ± SD, n = 3. Significant differences in **bold**

	R	R_BD	p-value	Day
(a) Seston				
Total suspended solids (mg l^{-1})	14.63 ± 0.88	62.02 ± 0.65	**0.0012**	2–27
Particulate inorganic matter (mg l^{-1})	8.59 ± 0.74	40.91 ± 0.89	**0.0018**	2–27
Particulate organic matter (mg l^{-1})	6.11 ± 0.15	21.11 ± 0.26	**0.0009**	2–27
Ratio particulate organic matter:particulate inorganic matter	0.88 ± 0.17	0.61 ± 0.06	0.0994	2–27
Percent particulate inorganic matter	57.55 ± 2.35	63.21 ± 1.67	0.1561	2–27
(b) Chl *a*, phaeophytin				
Chlorophyll *a* (µg l^{-1})	8.53 ± 0.50	**17.73 ± 2.22**	**0.0094**	2–27
Phaeophytin (µg l^{-1})	3.20 ± 0.34	29.59 ± 1.40	**<0.001**	2–27
Ratio chl *a*:phaeophytin	4.05 ± 0.42	0.60 ± 0.06	**0.0045**	2–27
Ratio chl *a*:particulate carbon	0.0107 ± 0.003	0.0277 ± 0.0062	**0.0239**	3–27
(c) Particulates				
Particulate phosphorus (µmol l^{-1})	0.55 ± 0.04	4.94 ± 0.18	**0.0015**	2–27
Particulate carbon (µmol l^{-1})	80.12 ± 12.01	545.80 ± 35.06	**0.0014**	2–27
Particulate nitrogen (µmol l^{-1})	10.12 ± 0.71	65.20 ± 3.65	**<0.001**	2–27
Ratio particulate carbon:particulate nitrogen	8.25 ± 0.71	8.04 ± 0.11	0.8126	2–27
(d) Dissolved nutrients, dissolved organic carbon, dissolved oxygen				
Ammonium	0.41 ± 0.07	0.54 ± 0.07	0.2108	2–27
Nitrate + nitrite (µmol l^{-1})	1.15 ± 0.22	5.35 ± 2.73	**0.0488**	2–27
Total dissolved nitrogen (µmol l^{-1})	23.44 ± 0.72	28.52 ± 3.57	**0.0214**	2–27
Dissolved inorganic nitrogen (µmol l^{-1})	1.55 ± 0.18	5.89 ± 2.69	**0.0455**	2–27
Dissolved organic nitrogen (µmol l^{-1})	21.88 ± 0.59	22.63 ± 1.43	0.5117	2–27
Total dissolved phosphorus (µmol l^{-1})	0.37 ± 0.008	0.87 ± 0.18	**0.0231**	2–27
Phosphate (µmol l^{-1})	0.08 ± 0.003	0.45 ± 0.14	0.0685	2–27
Dissolved organic phosphorus (µmol l^{-1})	0.29 ± 0.006	0.42 ± 0.05	**0.0124**	2–27
Dissolved organic carbon (µmol l^{-1})	180.65 ± 11.85	181.34 ± 8.78	0.9587	2–27
Dissolved silica (µmol l^{-1})	19.76 ± 3.15	26.57 ± 6.87	0.4439	2–27
Ratio dissolved inorganic nitrogen:dissolved inorganic phosphate	17.90 ± 0.89	15.31 ± 0.91	0.6388	2–27
Ratio dissolved silicate:phosphate	244.06 ± 40.02	186.96 ± 44.58	0.5652	2–27
Dissolved oxygen (mg l^{-1})	7.15 ± 0.20	4.73 ± 0.14	**0.0009**	1–28
(e) Total nutrients				
Total nitrogen (µmol l^{-1})	33.56 ± 1.40	93.72 ± 1.83	**<0.001**	2–27
Total phosphorus (µmol l^{-1})	0.92 ± 0.04	5.80 ± 0.02	**0.0016**	2–27
Ratio total nitrogen:total phosphorus	36.74 ± 1.09	18.32 ± 0.35	**<0.0001**	2–27
(f) Irradiance				
Irradiance at sediment surface (µmol photons m^{-2} s^{-1})	154.85 ± 9.67	3.68 ± 2.09	**0.0003**	2–27
Geometric mean irradiance (µmol photons m^{-2} s^{-1})	255.84 ± 2.91	26.94 ± 7.34	**0.0002**	2–27
(g) Zooplankton				
Adult *Acartia* sp. (ind. l^{-1})	3.70 ± 2.69	12.40 ± 7.17	**0.0247**	3–28
Copepodites (ind. l^{-1})	3.73 ± 1.61	7.24 ± 3.50	0.1501	3–28
Copepod nauplii (ind. l^{-1})	52.90 ± 11.63	82.21 ± 23.67	0.2338	3–28
Polychaete larvae (ind. l^{-1})	14.27 ± 9.64	1.91 ± 1.18	0.0793	3–28
Zooplankton carbon	5.11 ± 2.58	10.88 ± 5.22	**0.0277**	3–28

Phytoplankton, light, microphytobenthos

Water column chl *a* levels (10 to 30 µg l^{-1}) were significantly higher in the R_BD tanks than in the R tanks (8–12 µg l^{-1}) but decreased in the R_BD tanks after Day 15 to the end of the experiment (Fig. 6b, Table 1). Chl *a* levels decreased, in particular, in the R_BD tanks that had generated high concentrations of tunicates. Chl *a* did not substantially resuspend and settle in the R_BD and R tanks (Fig. 6f) as chl *a* concentrations were the same during the mixing 'on' and 'off' phases. Phaeophytin concentrations differed significantly between the mixing 'on' and the mixing 'off' phases as degraded material was resuspended and deposited in the R_BD tanks but not in the R tanks (Fig. 6c,g). The ratio of chl *a* to phaeophytin

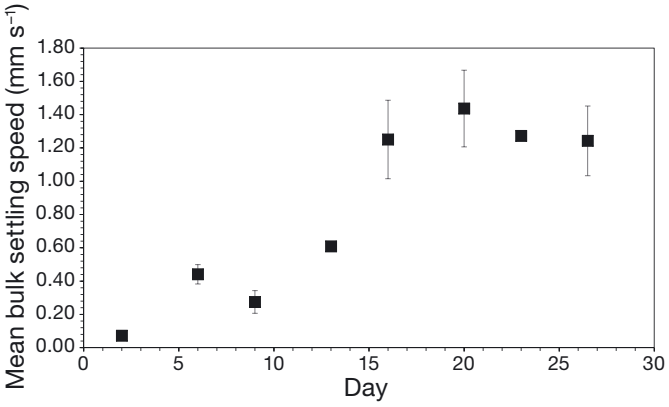

Fig. 7. Mean (± SD) bulk settling speeds in the R_BD tanks over the experiment (n = 3)

increased linearly in the R_BD tanks and was ~8-fold higher in the R_BD compared to the R tanks towards the end of the experiment (Fig. 6d,h, Table 1).

Phytoflagellates, cyanobacteria, dinoflagellates, and diatoms were present in all tanks. The tanks initially were dominated by phytoflagellates in low-moderate densities, but as the experiment progressed, diatoms became the dominant group in moderate-high densities. Many of the phytoflagellates were unidentifiable taxa but included *Cryptomonas* and *Pyramimonas*. The diatom taxa were dominated by the genus *Cyclotella* and included moderate numbers of *Thalassionema nitzschiodes*, *Cylindrotheca closterium*, and *Skeletonmea costatum*. The densities of dinoflagellates were very low throughout the experiment, and there were moderate numbers of an unidentified filamentous cyanobacteria (likely *Oscillatoria*).

While chl *a* concentrations were significantly higher in the R_BD tanks than in the R tanks (Fig. 5c), phytoplankton biomass as determined by direct cell counts converted to carbon was not significantly different between tanks (Fig. 9a). In addition, dinoflagellate (Fig. 9b), diatom (Fig. 9c) cyanobacteria (Fig. 9d), and phytoflagellate (Fig. 9e) abundances were similar, although they diverged after Day 20 with phytoflagellates, cyanobacteria, and dinoflagel-

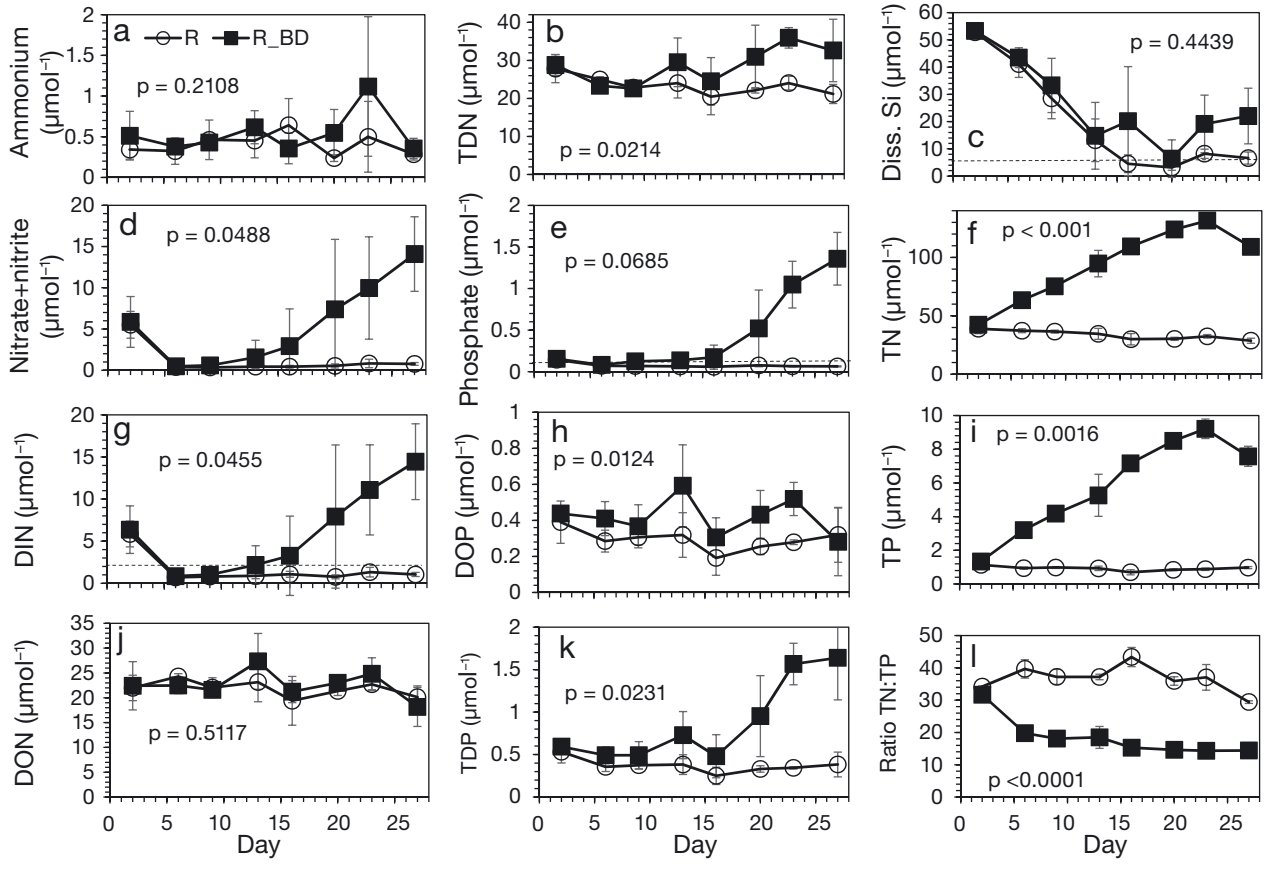

Fig. 8. Time series of nutrients, means and SD (n = 3) of (a) ammonium, (b) total dissolved nitrogen (TDN), (c) dissolved silicate, (d) nitrate + nitrite, (e) phosphate, (f) total nitrogen, (g) dissolved inorganic nitrogen (DIN), (h) dissolved organic phosphorus (DOP), (i) total phosphorus (TP), (j) dissolved organic nitrogen (DON), (k) total dissolved phosphorus (TDP) and (l) ratio of total nitrogen:total phosphorus over the experiment. Means ± SD (n = 3)

lates more abundant in the R_BD tanks. Diatoms decreased after Day 15 in the R_BD tanks until the end of the experiment (Fig. 9c), especially in the tanks where a high density of tunicates was found at the end of the experiment. Interestingly, if data from Day 2 (up to which point no biodeposits had yet been added) is excluded, the ratio of chl *a*:carbon is significantly higher in the R_BD tanks (Fig. 9f).

Light, as measured by a home-made Secchi disk, penetrated ~30 cm into the R_BD tanks during resuspension (Fig. 10b). During the off phases, Secchi depth in the R_BD tanks reached to 60 cm from Day 5 to 12 and then increased to 90 cm, occasionally reaching the bottom during the second phase of the experiment (Fig. 10b) which coincided with an increased bulk settling speed (Fig. 7). During that time, the water column became visually clearer in the R_BD tanks shortly after mixing 'off' (Fig. 10b). In contrast, in the R tanks, Secchi depth reached ~90 cm into the water column from Day 2 to 12 and reached to the bottom during the remainder of the experiment. At all times, Secchi depths reached the bottom during the mixing 'off' phases in the R tanks (Fig. 10b).

Measured bottom irradiance levels during the resuspension phase were low in the R_BD tanks that had high TSS concentrations (Fig. 10a). Irradiance at the sediment surface with ~150 µmol m^{-2} s^{-1} was higher in the R than in the R_BD systems (Fig. 10a, Table 1), and geometric mean irradiance in the water column was higher in the R tanks with ~250 µmol m^{-2} s^{-1} than in the R_BD tanks with ~10 µmol m^{-2} s^{-1} (Fig. S3 in the Supplement, Table 1).

Microphytobenthos grew on the fiberglass tank bottoms of the R tanks even though bottom shear stress was high with ~0.62 Pa. Qualitatively, microphytobenthos biomass was larger in the R tanks, which had significantly more light at the bottom, with high variability amongst the R tanks (Fig. 11a). Problems with the sampling container for microphytobenthos likely led to an underestimate of microphytobenthos chl *a* in the R tanks and the high variability. Percent degradation was significantly higher in R_BD tanks (Fig. 11b). The ratios of Fucoxanthin:chl *a*, Peridini:chl *a* and Lutein:chl *a* of the microphytobenthos were significantly larger in the R_BD tanks that had lower light at the bottom (Fig. S4 in the Supplement). The levels of 19′ Butanoyloxyfucoxanthin

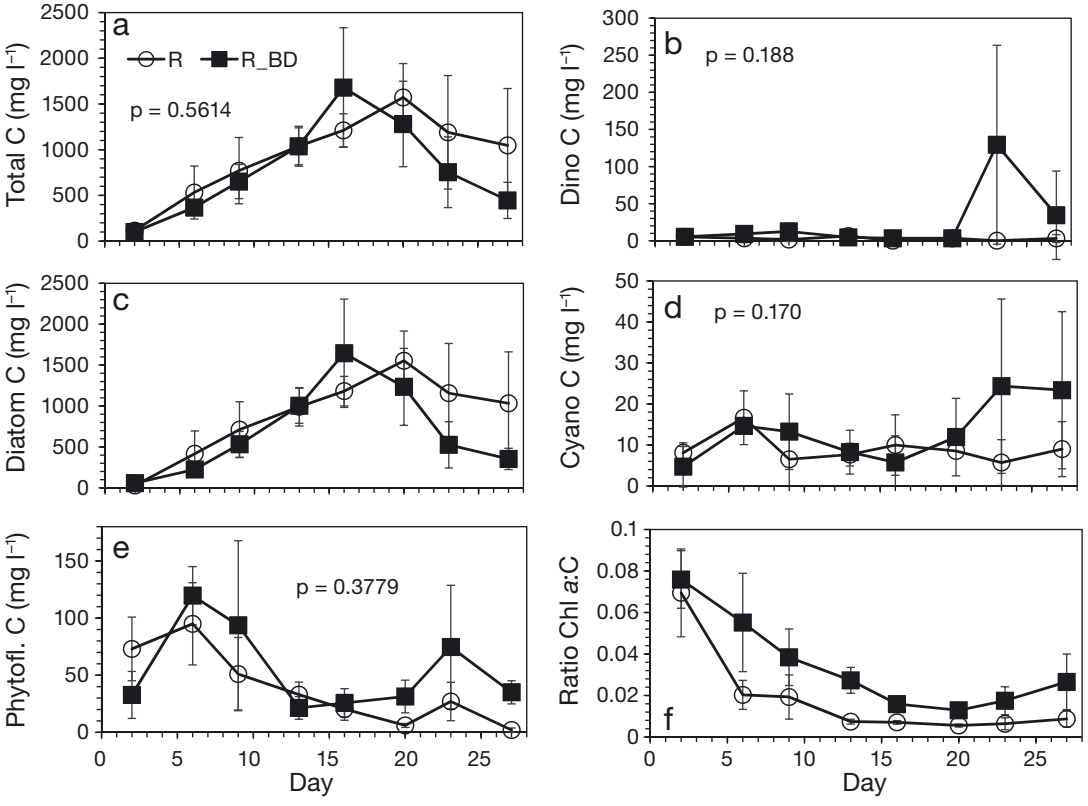

Fig. 9. Phytoplankton carbon (C) determined from direct cell counts, means ± SD (n = 3) for (a) total phytoplankton, (b) dino (dinoflagellates), (c) diatoms, (d) cyano (cyanobacteria), and (e) phytofl. (phytoflagellates). (f) Ratio of chlorophyll *a* to total phytoplankton C

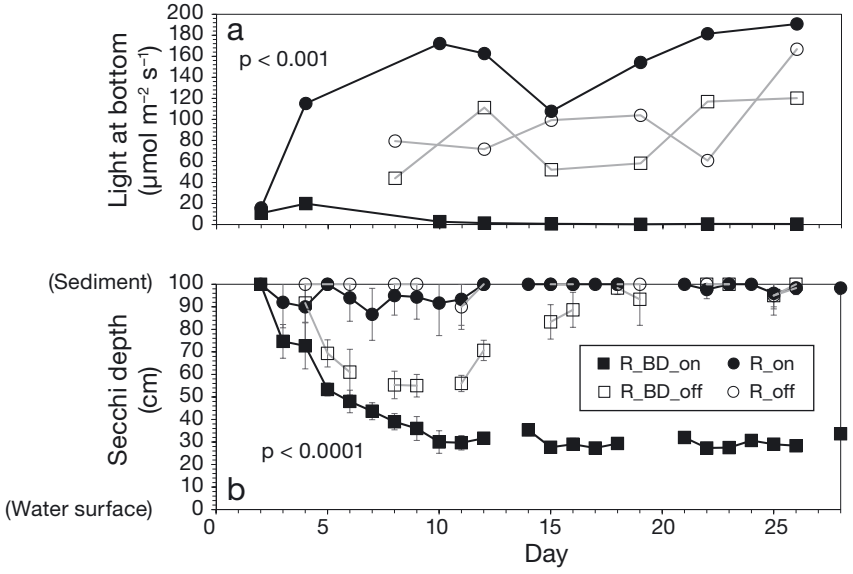

Fig. 10. (a) Light at the bottom during the mixing 'on' and 'off' phases of the experiment. (b) Secchi depth during the mixing 'on' and 'off' phases over the experiment

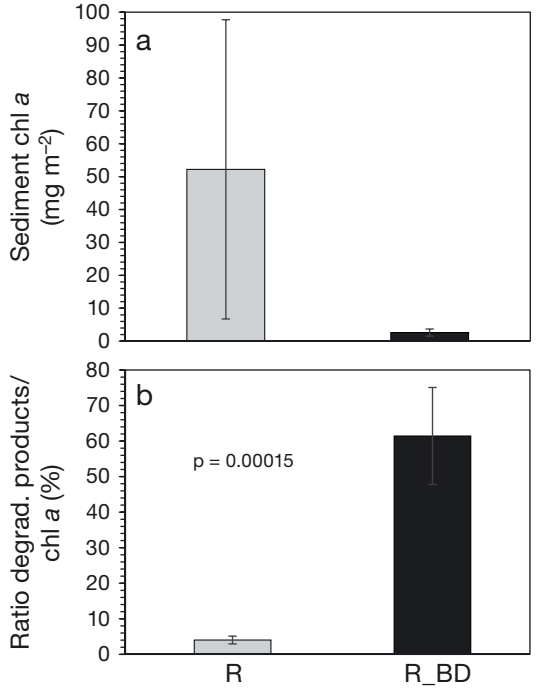

Fig. 11. (a) Sediment chlorophyll *a* at the end of the experiment in the R and R_BD tanks. (b) Ratio of degradation products (phaeophorbide + phaeophytin) to chl *a* in the microphytobenthos mats of the R and R_BD tanks. Means and SD (n = 3)

and Alloxanthin showed trends of being higher in the R_BD tanks, and Violaxanthin showed a trend of being higher in the R tanks (0.1> p > 0.05). None of the other pigment ratios were significantly different between the R and R_BD tanks.

Mesozooplankton and macrofauna

At the end of the experiment, 20 ± 5 m^{-2} adult polychaetes were found in the R tanks, some with established burrows in the microphytobenthos mat, and none in the R_BD tanks. Two R_BD tanks had 228 and 222 m^{-2} tunicates *Molgula manhattensis*, that filtered 449 and 437 l d^{-1}, respectively, in the second half of the experiment, however, 1 R_BD tank had only 2 tunicates in it that filtered 4 l d^{-1}. In the R tanks, 4 ± 7 m^{-2} tunicates were found that filtered 8 ± 14 l d^{-1} in the second half of the experiment. Moreover, 8 ± 7 m^{-2} small crabs were discovered in the R_BD tanks and none in the R tanks. Chl *a* concentrations and diatom biomass decreased greatly after Day 15 in the 2 R_BD tanks with a high density of tunicates.

Dominant mesozooplankton taxa found in the water column were adult *Acartia* sp. copepods (Fig. 12a), copepodites (Fig. 12b), copepod nauplii (Fig. 12c), and polychaete larvae (Fig. 12d). The pumps likely destroyed the adult mesozooplankton stages (Adey & Loveland 1998) during the initial raw water fill of the tanks at the start of the experiment, and it took ~1 wk until adult copepods and 16 d until polychaete larvae were found (Fig. 12a,d). The R_BD tanks contained ~15 adult *Acartia* sp. l^{-1} in the middle of the experiment and 25 at the end, while the R tanks contained 5 and 1, respectively. After 3 wk, *Acartia* sp. abundance decreased in all systems during a heat wave when copepods potentially migrated towards the bottom of the tank, but increased again on Day 24 in the R_BD tanks. Starting on Day 16 to the end, polychaete abundance was significantly (p = 0.045) higher in the R tanks (40 l^{-1}) than in the R_BD tanks (4 l^{-1}) and showed a trend (p = 0.0793) even when the first part of the experiment was included in the statistical analyses. *Acartia* sp. abundances were significantly higher in the R_BD system than in the R systems as was zooplankton carbon of all mesozooplankton combined. Barnacle nauplii, barnacle cyprid, crab zoea, and bivalve veliger larvae abundances were not significantly different between the R and R_BD tanks. Linear regression analysis showed no significant relation between phytoplankton biomass (from phytoplankton identifications) and zooplankton biomass (both converted to carbon units).

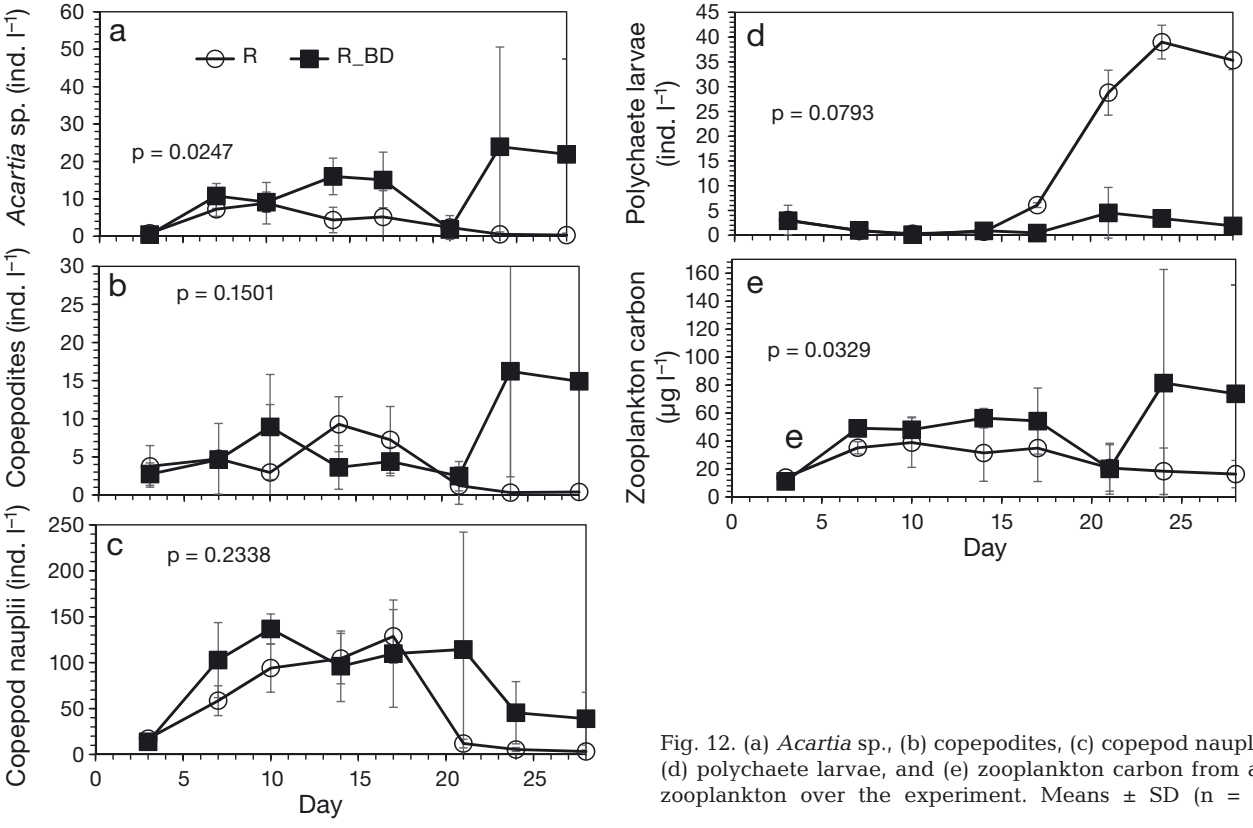

Fig. 12. (a) *Acartia* sp., (b) copepodites, (c) copepod nauplii, (d) polychaete larvae, and (e) zooplankton carbon from all zooplankton over the experiment. Means ± SD (n = 3)

Nitrogen budget

Zooplankton, phytoplankton biomass, microphytobenthos, and TDN were included in the nitrogen budget percentage estimations. An additional 0.77 g nitrogen per tank was found in the biodeposits in the R_BD tanks. The data in Table 2 suggest that biodeposit addition and tidal resuspension significantly affected nitrogen partitioning within the system. The R_BD system accumulated more nitrogen with 0.57 g N per tank for zooplankton nitrogen, phytoplankton nitrogen, microphytobenthos nitrogen and TDN; there was also an additional 0.77 g biodeposit particulate nitrogen (making a total of 1.34 g N per R_BD tank as compared to the R tanks with 1.02 g N per R tank). In the R tanks, all particulate nitrogen was composed of zooplankton nitrogen and phytoplankton nitrogen, while in the R_BD tanks, 0.77 g nitrogen was due to other sources, i.e. the biodeposit additions. In the R tanks, microphytobenthos dominated the system with 51.5% of the nitrogen portion, and in the R_BD tanks, TDN dominated the system with 72.4% of the nitrogen pool of zooplankton, phytoplankton, microphytobenthos and TDN due to biodeposit addition and resuspension. Phytoplankton nitrogen was 21% in the R_BD tanks and 13.8% in the R tanks of the zooplankton, phytoplankton, microphytoplankton and TDN nitrogen pool. The zooplankton nitrogen portion was small with 2% in the R_BD tanks and 1% in the R tanks. A major nitrogen input was also due to water exchanges, and the daily water exchange inputs were identical between the R and the R_BD tanks. Some phytoplankton nitrogen was exported during the daily exchange in the R and R_BD tanks. As we did not have bottom sediments in the tanks, no nitrogen is partitioned to nutrient fluxes from the sediments and to porewater resuspension. While for the R tanks microphytobenthos dominated the nitrogen pool, in the R_BD tanks particulate nitrogen and total dissolved nitrogen dominated the nitrogen pool in addition to the particulate nitrogen in biodeposits.

Table 2. Nitrogen budget (g N per tank). All particulate nitrogen (PN) in the R tanks is zooplankton and phytoplankton. TDN: total dissolved nitrogen

	R (g N/tank)	R_BD (g N/tank)
Zooplankton	0.01	0.01
Phytoplankton	0.14	0.12
Microphytobenthos	0.53	0.03
TDN	0.35	0.41
Biodeposit PN	0.00	0.77
Total (g N per tank)	1.02	1.34

DISCUSSION

Oyster *Crassostrea virginica* biodeposit additions and high bottom shear stress affected TSS concentrations, particle settling, light, nutrient dynamics, oxygen concentrations, and zooplankton community structure and abundance through direct and indirect interactions. Temperatures were high in this outdoor mesocosm experiment, especially during the heat wave from Days 19 to 22, but temperatures measured in an adjacent shallow Patuxent River cove were similarly high.

It has been suggested that biodeposition may promote phytoplankton growth during periods of nitrogen limitation (Cranford et al. 2007). However, resuspended biodeposits and nutrients regenerated from it did not affect phytoplankton abundance and composition in this whole-ecosystem experiment as measured by direct cell counts. Phytoflagellates, cyanobacteria, dinoflagellates, and diatom cell counts were not significantly different between systems even though differences were found during Day 22 to the end of the experiment. Phytoplankton carbon concentrations were similar in both systems. However, chl *a* concentrations were significantly higher in the R_BD tanks than the R tanks, and the increase and decrease in chl *a* concentrations corresponded to regenerated nutrients. At the end of the experiment, 2, 228, and 222 m^{-2} tunicates *Molgula manhattensis* were found in the 3 R_BD tanks, respectively, and led to decreased chl *a* and diatom concentrations. Tunicates are efficient filter feeders, and Comeau et al. (2015) reported that in the presence of the solitary tunicate *Ciona intestinalis* or *Styela clava* on mussel farms, the demand for phytoplankton increases by 30 to 47% compared to non-tunicate scenarios. *M. manhattensis* is an even more efficient filter feeder than *C. intestinalis* (Randløv & Riisgård 1979).

The chl *a*:carbon ratio was significantly higher in R_BD tanks than in the R tanks (if the first day is excluded), which suggests an adaptation of the phytoplankton to the low light regime in the R_BD tanks by increasing their chl *a* content in the cells (Buchanan et al. 2005). In addition, collected biodeposits contained a small amount of chl *a* added to the tanks daily that needed correction.

Resuspension of biodeposits increased TSS in the water column of the R_BD tanks, which was also found by Hildreth (1980) and Colden et al. (2016). In addition, biodeposit resuspension increased PN and PP levels in the water column of the R_BD tanks, reduced light penetration to the bottom, and resulted in lower microphytobenthos biomass in the R_BD tanks compared to the R tanks. While the experiment was run without a sediment bottom, microphytobenthos formed in the R tanks even though shear stress was high and polychaetes built burrow structures in it. While microphytobenthos abundance was higher in the R tanks that had more light at the bottom, a high Fucoxanthin:chl *a* ratio in R_BD tanks indicated that the microphytobenthos mat was adapted to low light (Cibic et al. 2007).

Oyster biodeposit resuspension affected nutrient transformations, nutrient regeneration, and the nitrogen budget. While tunicate biodeposition can be significant (Haven & Morales-Alamo 1966, McKindsey et al. 2009, Qi et al. 2015) and vertical material fluxes and nutrient regeneration from it important (Lee et al. 2012), nutrient regeneration was similar between the 3 R_BD tanks that had 2, 228, and 222 tunicates, respectively, at the end of the experiment, and tunicate biodeposition is thought to not be the driving factor here.

While nutrients did not get regenerated right away, after ~2 wk nitrate + nitrite, phosphate, and DOP increased strongly in the R_BD tanks, where desorption from particles may have played a role, whereas nutrient concentrations remained low in the R tanks. High temperatures may have mediated nutrient regeneration. Sufficient biodeposits may have accumulated by 2 wk into the experiment to see an effect. The increase in nutrient regeneration coincided with a change in bulk settling speeds in the R_BD. While particles did not settle in the R tanks, bulk settling speed increased in the R_BD tanks after Day 16, which suggests both that biodeposit particles aggregate and that, as they become bigger and denser, their net sedimentation rate increases. As feces and pseudofeces aggregate, bivalves are known to increase material sinking rates (Kautsky & Evans 1987). Tunicates are also thought to have a strong influence on vertical material fluxes (Lee et al. 2012), but all 3 R_BD tanks with 2, 222 and 228 tunicates, respectively, had similar bulk settling speeds and the tunicates are thought to not have had a dominant effect here. TSS concentrations were higher during the second half of the experiment which could have contributed to increased aggregation and settling.

The nitrogen budget partitioned differently in the R compared to the R_BD tanks. While the largest portion was partitioned in microphytobenthos (51.5%) in the R tanks, the largest portion of non-biodeposit nitrogen was partitioned in total dissolved nutrients in the R_BD tanks (72.4%). Resuspended biodeposits increased nutrient concentrations and reduced light penetration to the bottom where microphytobenthos

could form. Some of the regenerated nutrients likely came from desorption of nutrients from nutrient rich particles.

Oyster biodeposit resuspension affected ecosystem processes such as the zooplankton community composition and abundance. Zooplankton carbon concentrations were significantly higher in R_BD tanks compared to R tanks, and *Acartia* sp. were significantly more abundant in the R_BD tanks. However, polychaete larvae were more abundant in the second half of the experiment in the R tanks, and adult polychaetes had built burrows in the the microphytobenthos mat in the R tanks by the end of the experiment. Many tunicates were found in 2 of the 3 R_BD tanks and decreased chl *a* concentrations and diatom biomass but did not affect nutrient regeneration and particle aggregation and settling significantly.

No study has evaluated the effect of continuous levels of biodeposition to simulate conditions in bivalve culture. Biodeposits are typically assumed to fall to the bottom and stay at the bottom with the sediment matrix (Newell et al. 2005, Kellogg et al. 2013). Enhanced sedimentation under shellfish aquaculture is well documented (Cranford et al. 2003). However, transport from the reef or aquaculture facilities may have far-reaching consequences for the nutrient and particle dynamics and the light regime. Chamberlain et al. (2001) concluded that variations in the dispersion of biodeposits caused by local currents affected differences in the organic enrichment of sediments and macrobenthic infaunal diversity at 2 aquaculture farms. Testa et al. (2015) concluded, using a sediment model, that it is important to consider biodeposit resuspension and transport in effectively removing oyster biodeposits from an aquaculture farm to prevent negative effects. Giles et al. (2009) found that it was important to simulate biodeposit erosion and decay where changes in the decay rate, a complex process, greatly affected fecal pellet density on the bottom as well as dispersal distances. Bivalve biodeposit erosion, settling velocity, and disaggregation rate and any effects on the ecosystem are poorly understood.

Nutrient budgets need to include biodeposit resuspension when evaluating the impact of oysters on eutrophication mitigation. For the calculation of oyster environmental benefits, the fraction of deposited material that is resuspended and the fraction of nitrogen diagenesis that undergoes subsequent denitrification must be known (Cerco 2015). Moreover, nutrient transformations in the water column from resuspended biodeposits must also be known. In our experiments, nitrate + nitrite were regenerated, which are needed for denitrification, but we did not measure denitrification. It is possible denitrification took place in the anaerobic environment of resuspended biodeposits. A current focus in the field is on the effect of biodeposits fueling biogeochemically driven nitrogen removal from sediments (Newell et al. 2002, Higgins et al. 2013, Kellogg et al. 2014); however, effects on the biogeochemistry due to biodeposit resuspension must be considered. Furthermore, it has been suggested that strategies to maximize tissue-based nitrogen removal will be particularly important where environmental conditions do not support substantial nitrogen removal through biogeochemical sediment processes (Dalrymple & Carmichael 2015), but these studies do not include the effects of biodeposit resuspension.

Impacts of biodeposit resuspension may not be immediate: it took ~2 wk for effects to appear in this experiment, and short-term experiments will not capture these effects. Thus, experiments must have long enough duration to make sure that the system is in equilibrium, including biodeposit resuspension.

The experiments reported here did not include a sediment bottom and primarily focused on water column processes as mediated by biodeposit resuspension. Further changes can be expected when a muddy sediment bottom is included and thus sediment resuspension and interaction with biodeposits are included as well as sediment nutrient and gas fluxes. Existing studies of sediment resuspension and benthic processes have shown that sediment resuspension not only enhances nutrient fluxes from sediments (Qin et al. 2004, Almroth et al. 2009, Corbett 2010, Porter et al. 2010, Almroth-Rosell et al. 2012) but also significantly affects microbial and planktonic communities, and thus ultimately biogeochemical cycles (Porter et al. 2010, Wainright 1987, 1990, Isobe & Ohte 2014). Despite this limitation, this study contributed to the understanding of the effect of biodeposit addition and resuspension on the nutrient dynamics and ecosystem processes. Future studies will examine further effects of the interaction of resuspended biodeposits and sediments.

This study did not include actual oysters in the tanks. Additional well-known effects of oyster filtration include changes to phytoplankton biomass, seston concentration, and light penetration to the sediments (Porter et al. 2004b, Newell & Koch 2004). However, the focus in this experiment was on the less studied resuspended biodeposits that are difficult to track in nature (Testa et al. 2015) and cannot be resuspended in typical experimental ecosystem experiments with low bottom shear stress (Doering et al.

1986, Porter et al. 2010). The STURM facility allows high bottom shear stress for the tidal resuspension of biodeposits with realistic water column turbulence levels for benthic-pelagic coupling experiments (Porter et al. 2010, 2013), so that the focus could be on biodeposits, exclusively. Addition and regular tidal resuspension of oyster biodeposits profoundly affected nutrient dynamics, nitrogen partitioning, and zooplankton dynamics in this experiment.

Acknowledgements. We thank the University of Baltimore Foundation for funding, Eric Robins for help in the running of this experiment, and the Chesapeake Biological Laboratory and Horn Point Laboratory Analytical Services laboratories for sample analyses. We thank Kelton Clark for the use of his oysters and thank the Patuxent Environmental and Aquatic Research Laboratory for providing space and research support throughout this study. Presently, the University of Baltimore operates the STURM facility through a cooperative arrangement with the Patuxent Environmental and Aquatic Research Laboratory, Morgan State University. William Yates is thanked for his help with the seawater system. We thank 3 anonymous reviewers who provided constructive feedback.

LITERATURE CITED

Adey WH, Loveland K (1998) Pumps. In: Adey WH, Loveland K (ed) Dynamic aquaria, building living ecosystems. Academic Press, San Diego, p 27–33

Almroth E, Tengberg A, Andersson JH, Pakhomova S, Hall POJ (2009) Effects of resuspension on benthic fluxes of oxygen, nutrients, dissolved inorganic carbon, iron and manganese in the Gulf of Finland, Baltic Sea. Cont Shelf Res 29:807–818

Almroth-Rosell E, Tengberg A, Andersson S, Apler A, Hall POJ (2012) Effects of simulated natural and massive resuspension on benthic oxygen, nutrient and dissolved inorganic carbon fluxes in Loch Creran, Scotland. J Sea Res 72:38–48

Asmus RM, Asmus H (1991) Mussel beds: limiting or promoting phytoplankton? J Exp Mar Biol Ecol 148:215–232

Bayne BL, Hawkins AJS (1992) Ecological and physiological aspects of herbivory in benthic suspension-feeding molluscs. In: John DM, Hawkins SJ, Price JH (eds) Plant-animal interactions in the marine benthos. Systematics Association Special Vol 46. Clarendon Press, Oxford, p 265–288

Berg JA, Newell RIE (1986) Temporal and spatial variations in the composition of seston available to the suspension feeder *Crassostrea virginica.* Estuar Coast Shelf Sci 23: 375–386

Buchanan C, Lacouture RV, Marshall HG, Olson M, Johnson JM (2005) Phytoplankton reference communities for Chesapeake Bay and its tidal tributaries. Estuaries 28: 138–159

Caffrey JM, Sloth NP, Kaspar HF, Blackburn TH (1993) Effect of organic loading on nitrification and denitrification in a marine sediment microcosm. FEMS Microbiol Ecol 12:159–167

Cerco CF (2015) A multi-module approach to calculation of Oyster (*Crassostrea virginica*) environmental benefits. Environ Manage 56:467–479

Cerco CF, Noel MR (2007) Can oyster restoration reverse cultural eutrophication in Chesapeake Bay? Estuaries Coasts 30:331–343

Chamberlain J, Fernandes TF, Read P, Nickell TD, Davies IM (2001) Impacts of biodeposits from suspended mussel (*Mytilus edulis* L.) culture on the surrounding surficial sediments. ICES J Mar Sci 58:411–416

Chen CC, Petersen JE, Kemp WM (1997) Spatial and temporal scaling of periphyton growth on walls of estuarine mesocosms. Mar Ecol Prog Ser 155:1–15

Chesapeake Biological Laboratory Analytical Services Laboratory (2017a) University of Maryland Center for Environmental Science, water column chemistry methods. http://nasl.cbl.umces.edu/methods/WCC.html (accessed 9 September 2017)

Chesapeake Biological Laboratory Analytical Services Laboratory (2017b) Science, particulates and sediment methods. http://nasl.cbl.umces.edu/methods/PS.html (accessed 9 September 2017)

Cibic T, Blasutto O, Hancke K, Johnsen G (2007) Microphytobenthic species composition, pigment concentration, and primary production in sublittoral sediments of the Trondheimsfjord (Norway) 1. J Phycol 43:1126–1137

Cloern JE (1982) Does the benthos control phytoplankton biomass in south San Francisco Bay? Mar Ecol Prog Ser 9:191–202

Cohen RRH, Dresler PV, Phillips EJP, Cory RL (1984) The effect of the Asiatic clam, *Corbicula fluminea*, on phytoplankton of the Potomac River, Maryland. Limnol Oceanogr 29:170–180

Colden AM, Fall KA, Cartwright GM, Friedrichs CT (2016) Sediment suspension and deposition across restored oyster reefs of varying orientation to flow: implications for restoration. Estuaries Coasts 39:1435–1448

Comeau LA, Filgueira R, Guyondet T, Sonier R (2015) The impact of invasive tunicates on the demand for phytoplankton in longline mussel farms. Aquaculture 441: 95–105

Corbett DR (2010) Resuspension and estuarine nutrient cycling: insights from the Neuse River Estuary. Biogeosci 7:3289–3300

Cranford PJ, Dowd M, Grant J, Hargrave B, McGladdery S (2003) Ecosystem level effects of bivalve aquaculture. In: Can Tech Rep Fish Aquat Sci 2450:51–95

Cranford PJ, Strain PM, Dowd M, Hargrave BT, Grant J, Archambault M (2007) Influence of mussel aquaculture on nitrogen dynamics in a nutrient enriched coastal embayment. Mar Ecol Prog Ser 347:61–78

Dalrymple DJ, Carmichael RH (2015) Effects of age class on N removal capacity of oysters and implications for bioremediation. Mar Ecol Prog Ser 528:205–220

Dame RF (1996) Ecology of marine bivalves: an ecosystem approach. CRC Press, Boca Raton, FL

Dame RF, Libes S (1993) Oyster reefs and nutrient retention in tidal creeks. J Exp Mar Biol Ecol 171:251–258

Dame R, Zingmark R, Stevenson H, Nelson D (1980) Filter feeder coupling between the estuarine water column and benthic subsystems. Proc 5th Biennial Int Estuar Res Conf, Jekyll Island, Georgia, 7–12 October 1979. Academic Press, New York, NY, p 521–526

Dame RF, Spurrier JD, Wolaver TG (1989) Carbon, nitrogen and phosphorus processing by an oyster reef. Mar Ecol Prog Ser 54:249–256

Dame R, Dankers N, Prins T, Jongsma H, Smaal A (1991) The influence of mussel beds on nutrients in the Western Wadden Sea and Eastern Scheldt estuaries. Estuaries 14: 130–138

Doering PH, Oviatt CA, Kelly JR (1986) The effects of the filter-feeding clam *Mercenaria mercenaria* on carbon cycling in experimental marine mesocosms. J Mar Res 44:839–861

Enoksson V (1993) Nutrient recycling by coastal sediments: effects of added algal material. Mar Ecol Prog Ser 92: 245–254

Fisher TR, Peele ER, Ammerman JW, Harding LW (1992) Nutrient limitation of phytoplankton in Chesapeake Bay. Mar Ecol Prog Ser 82:51–63

Fisher TR, Gustafson AB, Sellner K, Lacouture R and others (1999) Spatial and temporal variation of resource limitation in Chesapeake Bay. Mar Biol 133:763–778

Giles H, Broekhuizen N, Bryan KR, Pilditch CA (2009) Modelling the dispersal of biodeposits from mussel farms: the importance of simulating biodeposit erosion and decay. Aquaculture 291:168–178

Grant WD, Williams AJ III, Glenn SM (1984) Bottom stress estimates and their prediction on the Northern California Continental Shelf during CODE-I: the importance of wave-current interaction. J Phys Oceanogr 14:506–527

Gross TF, Williams AJ, Terray EA (1994) Bottom boundary layer spectral dissipation estimates in the presence of wave motions. Cont Shelf Res 14:1239–1256

Gust G (1988) Skin friction probes for field applications. J Geophys Res, C, Oceans 93:14121–14132

Hargrave BT, Holmer M, Newcombe CP (2008) Towards a classification of organic enrichment in marine sediments based on biogeochemical indicators. Mar Pollut Bull 56: 810–824

Haven DS, Morales-Alamo R (1966) Aspects of biodeposition by oysters and other invertebrate filter feeders. Limnol Oceanogr 11:487–498

Haven DS, Morales-Alamo R (1970) Filtration of particles from suspension by the American oyster *Crassostrea virginica.* Biol Bull 139:248–264

Heathershaw AD (1976) Measurements of turbulence in the Irish Sea benthic boundary layer. In: McCave IN (ed) The benthic boundary layer. Plenum Press, New York, NY p 11–32

Higgins CB, Tobias C, Piehler MF, Smyth AR, Dame RF, Stephenson K, Brown BL (2013) Effect of aquacultured oyster biodeposition on sediment N_2 production in Chesapeake Bay. Mar Ecol Prog Ser 473:7–27

Hildreth DJ (1980) Bioseston production by *Mytilus edulis* and its effect in experimental systems. Mar Biol 55: 309–315

Isobe K, Ohte N (2014) Ecological perspectives on microbes involved in N-cycling. Microbes Environ 29:4–16

Johnson GC, Lueck RG, Sanford TB (1994) Stress on the Mediterranean outflow plume: Part 2. Turbulent dissipation and shear measurements. J Phys Oceanogr 24: 2084–2092

Jordan SJ (1987) Sedimentation and remineralization associated with biodeposition by the American oyster *Crassostrea virginica*. PhD dissertation, University of Maryland, College Park, MD

Karakassis I, Tsapakis M, Hatziyanni E (1998) Seasonal variability in sediment profiles beneath fish farm cages in the Mediterranean. Mar Ecol Prog Ser 162:243–252

Kautsky N, Evans S (1987) Role of biodeposition by *Mytilus edulis* in the circulation of matter and nutrients in a Baltic coastal ecosystem. Mar Ecol Prog Ser 38:201–212

Kellogg ML, Cornwell JC, Owens MS, Paynter KT (2013) Denitrification and nutrient assimilation on a restored oyster reef. Mar Ecol Prog Ser 480:1–19

Kellogg ML, Smyth AR, Luckenbach MW, Carmichael RH and others (2014) Use of oysters to mitigate eutrophication in coastal waters. Estuar Coast Shelf Sci 151:156–168

Lacouture RV (2001) Quality assurance documentation plan for the phytoplankton component of the Chesapeake Bay water quality monitoring program. Report prepared for the Maryland Department of Natural Resources by the Academy of Natural Sciences Estuarine Research Center, available at http://chesapeakebay.net/data/index.htm

Lee JS, Kim SH, Shin KH, Hyun JH, Kim SY (2012) Influence of sea squirt (*Halocynthia roretzi*) aquaculture on benthic-pelagic coupling in coastal waters: a study of the South Sea in Korea. Estuar Coast Shelf Sci 99:10–20

Liu JH, Yang SL, Zhu Q, Zhang J (2014) Controls on suspended sediment concentration profiles in the shallow and turbid Yangtze Estuary. Cont Shelf Res 90:96–108

Lund EJ (1957) Self silting, survival of the oyster as a closed system and reducing tendencies of the environment of the oyster. Publ Inst Mar Sci Univ Tex 4:313–319

MacIntyre HL, Geider RJ, Miller DC (1996) Microphytobenthos: the ecological role of the 'secret garden' of unvegetated, shallow-water marine habitats. I. Distribution, abundance and primary production. Estuaries 19:186–201

Marshall HG, Alden RW (1990) Spatial and temporal diatom assemblages and other phytoplankton within the lower Chesapeake Bay, USA. In: Simola H (ed) Proceedings of the 10th International Diatom Symposium. Koeltz Scientific Books, Koenigstein, p 311–322

Mason RP, Porter ET (2009) Toxicity and bioaccumulation in benthic organisms. In: Petersen JE, Kennedy VS, Dennison WC, Kemp WM (eds) Experimental ecosystems and scale. Tools for understanding and managing coastal ecosystems. Springer, New York, NY, p 203–211

McKindsey CW, Lecuona M, Huot M, Weise AM (2009) Biodeposit production and benthic loading by farmed mussels and associate epifauna in Prince Edward Island. Aquaculture 295:44–51

Millar RH (1971) The biology of ascidians, II Feeding. In: Russel FS, Yonge M (eds) Advances in marine biology, Vol 9. Academic Press, London, New York, NY, p 2–5

Newell RIE (1988) Ecological changes in Chesapeake Bay: are they the result of overharvesting the American oyster, *Crassostrea virginica*? In: Lynch MP, Krome EC (eds) Understanding the estuary: advances in Chesapeake Bay research. Chesapeake Research Consortium Publication, 129(CBP/TRS 24/88), Gloucester Point, VA, p 536–546

Newell RIE, Koch EW (2004) Modeling seagrass density and distribution in response to changes in turbidity stemming from bivalve filtration and seagrass sediment stabilization. Estuaries 27:793–806

Newell RIE, Cornwell JC, Owens MS (2002) Influence of simulated bivalve biodeposition and microphytobenthos on sediment nitrogen dynamics: a laboratory study. Limnol Oceanogr 47:1367–1379

Newell RIE, Fisher TR, Holyoke RR, Cornwell JC (2005) Influence of eastern oysters on nitrogen and phosphorus regeneration in Chesapeake Bay, USA. In: Dame RF, Olenin S (eds) The comparative roles of suspension feeders in ecosystems. Kluwer, Dordrecht, p 93–120

Officer CB, Smayda TJ, Mann R (1982) Benthic filter-feeding: a natural eutrophication control. Mar Ecol Prog Ser 9:203–210

Parsons TR, Maita Y, Lalli CM (1984) A manual of chemical and biological methods for seawater analysis. Pergamon, Oxford University Press, Oxford

Petersen JE, Sanford LP, Kemp WM (1998) Coastal plankton responses to turbulent mixing in experimental ecosystems. Mar Ecol Prog Ser 171:23–41

Piehler MF, Smyth AR (2011) Habitat-specific distinctions in estuarine denitrification affect both ecosystem function and services. Ecosphere 2:art12

Porter ET, Sanford LP, Gust G, Porter FS (2004a) Combined water-column mixing and benthic boundary-layer flow in mesocosms: key for realistic benthic-pelagic coupling studies. Mar Ecol Prog Ser 271:43–60

Porter ET, Cornwell JC, Sanford LP, Newell RIP (2004b) Effect of oysters *Crassostrea virginica* and bottom shear velocity on benthic-pelagic coupling and estuarine water quality. Mar Ecol Prog Ser 271:61–75

Porter ET, Mason RP, Sanford LP (2010) Effect of tidal resuspension on benthic–pelagic coupling in an experimental ecosystem study. Mar Ecol Prog Ser 413:33–53

Porter ET, Mason RP, Sanford LP (2013) Effects of shear stress and hard clams on seston, microphytobenthos, and nitrogen dynamics in mesocosms with tidal resuspension. Mar Ecol Prog Ser 479:25–45

Porter ET, Sanford LP, Porter FS, Mason RP (2018) STURM: resuspension mesocosms with realistic shear and turbulence for benthic-pelagic coupling studies: design and applications. J Exp Mar Biol Ecol 499:35–50

Qi Z, Han T, Zhang J, Huang H, Mao Y, Jiang Z, Fang J (2015) First report on in situ biodeposition rates of ascidians (*Ciona intestinalis* and *Styela clava*) during summer in Sanggou Bay, northern China. Aquacult Environ Interact 6:233–239

Qin B, Hu W, Gao G, Luo L, Zhang J (2004) Dynamics of sediment resuspension and the conceptual schema of nutrient release in the large shallow Lake Taihu, China. Chin Sci Bull 49:54–64

Randløv A, Riisgård HU (1979) Efficiency of particle retention and filtration rate in four species of ascidians. Mar Ecol Prog Ser 1:55–59

Ray NE, Li J, Kangas PC, Terlizzi DE (2015) Water quality upstream and downstream of a commercial oyster aquaculture facility in Chesapeake Bay, USA. Aquacult Eng 68:35–42

Sanford LP (1997) Turbulent mixing in experimental ecosystems. Mar Ecol Prog Ser 161:265–293

Sanford LP, Halka JP (1993) Assessing the paradigm of mutually exclusive erosion and deposition of mud, with examples from upper Chesapeake Bay. Mar Geol 114: 37–57

Sanford LP, Suttles SE, Porter ET (2009) Physical factors: mixing and flow. In: Petersen JE, Kennedy VS, Dennison WC, Kemp WM (eds) Enclosed experimental ecosystems and scale. Tools for understanding and managing coastal ecosystems. Springer, New York, NY, p 63–74

Schulte DM, Burke RP (2014) Recruitment enhancement as an indicator of oyster restoration success in Chesapeake Bay. Ecol Restor 32:434–440

Smayda TJ (1978) From phytoplankton biomass. In: Sournia A (ed) Phytoplankton manual. United Nations Educational, Scientific and Cultural Organization, Paris, p 273–279

Smyth AR, Thompson SP, Siporin KN, Gardner WS, McCarthy MJ, Piehler MF (2013) Assessing nitrogen dynamics throughout the estuarine landscape. Estuaries Coasts 36:44–55

Souchu P, Vaquer A, Collos Y, Landrein S, Deslous-Paoli JM, Bibent B (2001) Influence of shellfish farming activities on the biogeochemical composition of the water column in Thau lagoon. Mar Ecol Prog Ser 218:141–152

Sprung M (1984) Physiological energetics of mussel larvae (*Mytilus edulis*). I. Shell growth and biomass. Mar Ecol Prog Ser 17:283–293

Strathmann RR (1967) Estimating the organic carbon content of phytoplankton from cell volume or plasma volume. Limnol Oceanogr 12:411–418

Sundbäck K, Granéli W (1988) Influence of microphytobenthos on the nutrient flux between sediment and water: a laboratory study. Mar Ecol Prog Ser 43:63–69

Sundbäck K, Enoksson V, Granéli W, Pettersson K (1991) Influence of sublittoral microphytobenthos on the oxygen and nutrient flux between sediment and water: a laboratory continuous-flow study. Mar Ecol Prog Ser 74:263–279

Sundbäck K, Miles A, Goeransson E (2000) Nitrogen fluxes, denitrification and the role of microphytobenthos in microtidal shallow water sediments: an annual study. Mar Ecol Prog Ser 200:59–76

Tennekes H, Lumley JL (1972) A first course in turbulence. MIT Press, Cambridge, MA

Terray EA, Donelan MA, Agrawal YC, Drennan WM and others (1996) Estimates of kinetic energy dissipation under breaking waves. J Phys Oceanogr 26:792–807

Testa JM, Brady DC, Cornwell JC, Owens MS and others (2015) Modeling the impact of floating oyster (*Crassostrea virginica*) aquaculture on sediment-water nutrient and oxygen fluxes. Aquacult Environ Interact 7:205–222

Torres G, Giminez L, Anger K (2002) Effects of reduced salinity on the biochemical composition (lipid, protein) of zoea 1 decapod crustacean larvae. J Exp Mar Biol Ecol 277:43–60

Van Heukelem L, Thomas CS (2001) Computer-assisted high-performance liquid chromatography method development with applications to the isolation and analysis of phytoplankton pigments. J Chromatogr A 910:31–49

Wainright SC (1987) Stimulation of heterotrophic microplankton production by resuspended marine sediments. Science 238:1710–1712

Wainright SC (1990) Sediment-to-water fluxes of particulate material and microbes by resuspension and their contribution to the planktonic food web. Mar Ecol Prog Ser 62: 271–281

Welschmeyer NA (1994) Fluorometric analysis of chlorophyll *a* in the presence of chlorophyll *b* and phaeopigments. Limnol Oceanogr 39:1985–1992

White JR, Roman MR (1992) Seasonal study of grazing by metazoan zooplankton in the mesohaline Chesapeake Bay. Mar Ecol Prog Ser 86:251–261

Widdows J, Brinsley MD, Salkeld PN, Elliott M (1998) Use of annular flumes to determine the influence of current velocity and bivalves on material flux at the sediment-water interface. Estuaries 21:552–559

Williamson TR, Tilley DR, Campbell E (2015) Emergy analysis to evaluate the sustainability of two oyster aquaculture systems in the Chesapeake Bay. Ecol Eng 85:103–120

Wright LD, Boon JD, Xu JP, Kim SC (1992) The bottom boundary layer of the Bay Stem Plains environment of lower Chesapeake Bay. Estuar Coast Shelf Sci 35:17–36

Zimmerman CF, Keefe CW, Bashe J (1997) EPA Method 440.0. Determination of carbon and nitrogen in sediments and particulates of estuarine/coastal waters using elemental analysis. National Exposure Laboratory, Office of Research and Development, US Environmental Protection Agency, Cincinnati, OH. Available at https://cfpub.epa.gov/si/si_public_record_report.cfm?dirEntryId=309418 (accessed 9 September 2017)

Editorial responsibility: Just Cebrian, Dauphin Island, Alabama, USA

Submitted: April 11, 2017; Accepted: November 14, 2017
Proofs received from author(s): December 21, 2017